

## MINIMAL SUBMANIFOLDS

TOBIAS H. COLDING AND WILLIAM P. MINICOZZI II

## CONTENTS

1. Introduction	2
<b>Part 1. Classical and almost classical results</b>	<b>2</b>
1.1. The Gauss map	3
1.2. Minimal graphs	4
1.3. The maximum principle	5
2. Monotonicity and the mean value inequality	7
3. Rado's theorem	8
4. The theorems of Bernstein and Bers	9
5. Simons inequality	10
6. Heinz's curvature estimate for graphs	11
7. Embedded minimal disks with area bounds	11
8. Stable minimal surfaces	12
9. Regularity theory	13
9.1. $\epsilon$ -regularity and the singular set	14
9.2. Tangent cone analysis	14
<b>Part 2. Embedded minimal surfaces</b>	<b>15</b>
10.1. Multi-valued graphs	15
10.2. The sublinear growth of the separation	16
11. Embedded minimal disks	17
12. Fixed genus	20
12.1. Uniformly locally simply connected	20
12.2. Fixed genus	23
<b>Part 3. Global theory of minimal surfaces in <math>\mathbf{R}^3</math></b>	<b>25</b>
13.1. Minimal surfaces with finite total curvature	25
13.2. The uniqueness of the catenoid	25
14. Global theory of embedded minimal surfaces	25
15. The Calabi-Yau conjectures	27
<b>Part 4. Constructing minimal surfaces</b>	<b>29</b>
16. The Plateau Problem	29
17. The Weierstrass representation	30
18. Area-minimizing surfaces	31
19. The min-max construction of minimal surfaces	32

---

The authors were partially supported by NSF Grants DMS 0104453 and DMS 0405695.

<b>Part 5. Some applications of minimal surfaces</b>	33
20.1. The positive mass theorem	34
20.2. Black holes	35
20.3. Constant mean curvature surfaces	36
20.4. Finite extinction for Ricci flow	36
References	37

## 1. INTRODUCTION

In this article, we survey some old and new results about minimal surfaces and submanifolds. The field of minimal surfaces has its origin in the mid eighteenth century with the work of Euler and Lagrange but it has very recently seen major advances that have solved many long standing open conjectures in the field. In what follows, we give a quick tour through the field, starting with the definition and the classical results and ending up with current areas of research. Many references are given for further reading.

Soap films, soap bubbles, and surface tension were extensively studied by the Belgian physicist and inventor (the inventor of the stroboscope) Joseph Plateau in the first half of the nineteenth century. At least since his studies, it has been known that the right mathematical model for soap films are minimal surfaces – the soap film is in a state of minimum energy when it is covering the least possible amount of area. Minimal surfaces and equations like the minimal surface equation have served as mathematical models for many physical problems.

The field of minimal surfaces dates back to the publication in 1762 of Lagrange’s famous memoir “Essai d’une nouvelle méthode pour déterminer les maxima et les minima des formules intégrales indéfinies”. Euler had already in a paper published in 1744 discussed minimizing properties of the surface now known as the catenoid, but he only considered variations within a certain class of surfaces. In the almost one quarter of a millennium that has past since Lagrange’s memoir minimal surfaces has remained a vibrant area of research and there are many reasons why. The study of minimal surfaces was the birthplace of regularity theory. It lies on the intersection of nonlinear elliptic PDE, geometry, topology and general relativity.

### Part 1. Classical and almost classical results

Let  $\Sigma \subset \mathbf{R}^n$  be a smooth  $k$ -dimensional submanifold (possibly with boundary) and  $C_0^\infty(N\Sigma)$  the space of all infinitely differentiable, compactly supported, normal vector fields on  $\Sigma$ . Given  $\Phi$  in  $C_0^\infty(N\Sigma)$ , consider the one-parameter variation

$$(1.1) \quad \Sigma_{t,\Phi} = \{x + t\Phi(x) | x \in \Sigma\}.$$

The so called *first variation formula* of volume is the equation

$$(1.2) \quad \left. \frac{d}{dt} \right|_{t=0} \text{Vol}(\Sigma_{t,\Phi}) = \int_{\Sigma} \langle \Phi, \mathbf{H} \rangle,$$

where  $\mathbf{H}$  is the mean curvature (vector) of  $\Sigma$ . Here, and throughout this paper, integration is with respect to  $d\text{vol}$ . (When  $\Sigma$  is noncompact, then  $\Sigma_{t,\Phi}$  in (1.2) is

replaced by  $\Gamma_{t,\Phi}$ , where  $\Gamma$  is any compact set containing the support of  $\Phi$ .) The submanifold  $\Sigma$  is said to be a *minimal submanifold* (or just minimal) if

$$(1.3) \quad \left. \frac{d}{dt} \right|_{t=0} \text{Vol}(\Sigma_{t,\Phi}) = 0 \quad \text{for all } \Phi \in C_0^\infty(N\Sigma)$$

or, equivalently by (1.2), if the mean curvature  $\mathbf{H}$  is identically zero. Thus  $\Sigma$  is minimal if and only if it is a critical point for the volume functional. (Since a critical point is not necessarily a minimum the term “minimal” is misleading, but it is time honored. The equation for a critical point is also sometimes called the Euler–Lagrange equation.)

Suppose now, for simplicity, that  $\Sigma$  is an oriented hypersurface with unit normal  $\mathbf{n}_\Sigma$ . We can then write a normal vector field  $\Phi \in C_0^\infty(N\Sigma)$  as  $\Phi = \phi \mathbf{n}_\Sigma$ , where the function  $\phi$  is in the space  $C_0^\infty(\Sigma)$  of infinitely differentiable, compactly supported functions on  $\Sigma$ . Using this, a computation shows that if  $\Sigma$  is minimal, then

$$(1.4) \quad \left. \frac{d^2}{dt^2} \right|_{t=0} \text{Vol}(\Sigma_{t,\phi \mathbf{n}_\Sigma}) = - \int_\Sigma \phi L_\Sigma \phi,$$

where

$$(1.5) \quad L_\Sigma \phi = \Delta_\Sigma \phi + |A|^2 \phi$$

is the second variational (or Jacobi) operator. Here  $\Delta_\Sigma$  is the Laplacian on  $\Sigma$  and  $A$  is the second fundamental form. So  $|A|^2 = \kappa_1^2 + \kappa_2^2 + \cdots + \kappa_{n-1}^2$ , where  $\kappa_1, \dots, \kappa_{n-1}$  are the principal curvatures of  $\Sigma$  and  $\mathbf{H} = (\kappa_1 + \cdots + \kappa_{n-1}) \mathbf{n}_\Sigma$ . A minimal submanifold  $\Sigma$  is said to be *stable* if

$$(1.6) \quad \left. \frac{d^2}{dt^2} \right|_{t=0} \text{Vol}(\Sigma_{t,\Phi}) \geq 0 \quad \text{for all } \Phi \in C_0^\infty(N\Sigma).$$

Integrating by parts in (1.4), we see that stability is equivalent to the so called *stability inequality*

$$(1.7) \quad \int |A|^2 \phi^2 \leq \int |\nabla \phi|^2.$$

More generally, the *Morse index* of a minimal submanifold is defined to be the number of negative eigenvalues of the operator  $L$ . Thus, a stable submanifold has Morse index zero.

**1.1. The Gauss map.** Let  $\Sigma^2 \subset \mathbf{R}^3$  be a surface (not necessarily minimal). The *Gauss map* is a continuous choice of a unit normal  $\mathbf{n} : \Sigma \rightarrow \mathbf{S}^2 \subset \mathbf{R}^3$ . Observe that there are two choices  $\mathbf{n}$  and  $-\mathbf{n}$  corresponding to a choice of orientation of  $\Sigma$ . If  $\Sigma$  is minimal, then the Gauss map is an (anti) conformal map since the eigenvalues of the Weingarten map are  $\kappa_1$  and  $\kappa_2 = -\kappa_1$ . Moreover, for a minimal surface

$$(1.8) \quad |A|^2 = \kappa_1^2 + \kappa_2^2 = -2 \kappa_1 \kappa_2 = -2 K_\Sigma,$$

where  $K_\Sigma$  is the Gauss curvature. It follows that the area of the image of the Gauss map is a multiple of the total curvature.

**1.2. Minimal graphs.** Suppose that  $u : \Omega \subset \mathbf{R}^2 \rightarrow \mathbf{R}$  is a  $C^2$  function. The graph of  $u$

$$(1.9) \quad \text{Graph}_u = \{(x, y, u(x, y)) \mid (x, y) \in \Omega\}.$$

has area

$$(1.10) \quad \begin{aligned} \text{Area}(\text{Graph}_u) &= \int_{\Omega} |(1, 0, u_x) \times (0, 1, u_y)| \\ &= \int_{\Omega} \sqrt{1 + u_x^2 + u_y^2} = \int_{\Omega} \sqrt{1 + |\nabla u|^2}, \end{aligned}$$

and the (upward pointing) unit normal is

$$(1.11) \quad \mathbf{n} = \frac{(1, 0, u_x) \times (0, 1, u_y)}{|(1, 0, u_x) \times (0, 1, u_y)|} = \frac{(-u_x, -u_y, 1)}{\sqrt{1 + |\nabla u|^2}}.$$

Therefore for the graphs  $\text{Graph}_{u+t\eta}$  where  $\eta|_{\partial\Omega} = 0$  we get that

$$(1.12) \quad \text{Area}(\text{Graph}_{u+t\eta}) = \int_{\Omega} \sqrt{1 + |\nabla u + t \nabla \eta|^2},$$

hence

$$(1.13) \quad \begin{aligned} \left. \frac{d}{dt} \right|_{t=0} \text{Area}(\text{Graph}_{u+t\eta}) &= \int_{\Omega} \frac{\langle \nabla u, \nabla \eta \rangle}{\sqrt{1 + |\nabla u|^2}} \\ &= - \int_{\Omega} \eta \operatorname{div} \left( \frac{\nabla u}{\sqrt{1 + |\nabla u|^2}} \right). \end{aligned}$$

It follows that the graph of  $u$  is a critical point for the area functional if and only if  $u$  satisfies the divergence form equation

$$(1.14) \quad \operatorname{div} \left( \frac{\nabla u}{\sqrt{1 + |\nabla u|^2}} \right) = 0.$$

We will refer to (1.14) as the *minimal surface equation*.

Next we want to show that the graph of a function on  $\Omega$  satisfying the minimal surface equation is not just a critical point for the area functional but is actually area-minimizing amongst surfaces in the cylinder  $\Omega \times \mathbf{R} \subset \mathbf{R}^3$ . To show this, first extend first the unit normal  $\mathbf{n}$  of the graph in (1.11) to a vector field, still denoted by  $\mathbf{n}$ , on the entire cylinder  $\Omega \times \mathbf{R}$  by setting

$$(1.15) \quad \mathbf{n}(x, y, z) = \mathbf{n}(x, y, u(x, y)).$$

Let  $\omega$  be the two-form on  $\Omega \times \mathbf{R}$  given by the condition that for  $X, Y \in \mathbf{R}^3$

$$(1.16) \quad \omega(X, Y) = \det(X, Y, \mathbf{n}).$$

An easy calculation shows that

$$(1.17) \quad d\omega = \frac{\partial}{\partial x} \left( \frac{-u_x}{\sqrt{1 + |\nabla u|^2}} \right) + \frac{\partial}{\partial y} \left( \frac{-u_y}{\sqrt{1 + |\nabla u|^2}} \right) = 0,$$

since  $u$  satisfies the minimal surface equation. In sum, the form  $\omega$  is closed and, given any  $X$  and  $Y$  at a point  $(x, y, z)$ ,

$$(1.18) \quad |\omega(X, Y)| \leq |X \times Y|,$$

where equality holds if and only if

$$(1.19) \quad X, Y \subset T_{(x,y,u(x,y))} \text{Graph}_u .$$

Such a form  $\omega$  is called a *calibration*. From this, we have that if  $\Sigma \subset \Omega \times \mathbf{R}$  is any other surface with  $\partial\Sigma = \partial \text{Graph}_u$ , then by Stokes' theorem since  $\omega$  is closed,

$$(1.20) \quad \text{Area}(\text{Graph}_u) = \int_{\text{Graph}_u} \omega = \int_{\Sigma} \omega \leq \text{Area}(\Sigma) .$$

This shows that  $\text{Graph}_u$  is area-minimizing among all surfaces in the cylinder and with the same boundary.

If the domain  $\Omega$  is convex, the minimal graph is absolutely area-minimizing. To see this, observe first that if  $\Omega$  is convex, then so is  $\Omega \times \mathbf{R}$ , and hence the nearest point projection  $P : \mathbf{R}^3 \rightarrow \Omega \times \mathbf{R}$  is a distance nonincreasing Lipschitz map that is equal to the identity on  $\Omega \times \mathbf{R}$ . If  $\Sigma \subset \mathbf{R}^3$  is any other surface with  $\partial\Sigma = \partial \text{Graph}_u$ , then  $\Sigma' = P(\Sigma)$  has  $\text{Area}(\Sigma') \leq \text{Area}(\Sigma)$ . Applying (1.20) to  $\Sigma'$ , we see that  $\text{Area}(\text{Graph}_u) \leq \text{Area}(\Sigma')$  and the claim follows.

If  $\Omega \subset \mathbf{R}^2$  contains a ball of radius  $r$ , then, since  $\partial B_r \cap \text{Graph}_u$  divides  $\partial B_r$  into two components at least one of which has area at most  $(\text{Area}(\mathbf{S}^2)/2) r^2$ , we get from (1.20) the crude estimate

$$(1.21) \quad \text{Area}(B_r \cap \text{Graph}_u) \leq \frac{\text{Area}(\mathbf{S}^2)}{2} r^2 .$$

Very similar calculations to the ones above show that if  $\Omega \subset \mathbf{R}^{n-1}$  and  $u : \Omega \rightarrow \mathbf{R}$  is a  $C^2$  function, then the graph of  $u$  is a critical point for the area functional if and only if  $u$  satisfies (1.14). Moreover, as in (1.20), the graph of  $u$  is actually area-minimizing. Consequently, as in (1.21), if  $\Omega$  contains a ball of radius  $r$ , then

$$(1.22) \quad \text{Vol}(B_r \cap \text{Graph}_u) \leq \frac{\text{Vol}(\mathbf{S}^{n-1})}{2} r^{n-1} .$$

**1.3. The maximum principle.** The first variation formula, (1.2), showed that a smooth submanifold is a critical point for area if and only if the mean curvature vanishes. We will next derive the weak form of the first variation formula which is the basic tool for working with “weak solutions” (typically, stationary varifolds). Let  $X$  be a vector field on  $\mathbf{R}^n$ . We can write the divergence  $\text{div}_{\Sigma} X$  of  $X$  on  $\Sigma$  as

$$(1.23) \quad \text{div}_{\Sigma} X = \text{div}_{\Sigma} X^T + \text{div}_{\Sigma} X^N = \text{div}_{\Sigma} X^T + \langle X, \mathbf{H} \rangle ,$$

where  $X^T$  and  $X^N$  are the tangential and normal projections of  $X$ . In particular, we get that, for a minimal submanifold,

$$(1.24) \quad \text{div}_{\Sigma} X = \text{div}_{\Sigma} X^T .$$

Moreover, from (1.23) and Stokes' theorem, we see that  $\Sigma$  is minimal if and only if for all vector fields  $X$  with compact support and vanishing on the boundary of  $\Sigma$ ,

$$(1.25) \quad \int_{\Sigma} \text{div}_{\Sigma} X = 0 .$$

The key point is that (1.25) makes sense as long as we can define the divergence of a vector field on  $\Sigma$ .

The two most common notions of weakly minimal submanifolds are minimal currents and stationary varifolds. A *k-varifold*  $\Sigma$  on  $\mathbf{R}^n$  is a Radon measure on  $\mathbf{R}^n \times G(k, n)$ , where  $G(k, n)$  is the space of (unoriented)  $k$ -planes through the

origin in  $\mathbf{R}^n$  (so that  $G(n-1, n)$  is projective  $(n-1)$  space). If  $X$  is a  $C^1$  vector field, then we define the divergence with respect to  $(x, \omega) \in \mathbf{R}^n \times G(k, n)$  by

$$(1.26) \quad \operatorname{div}_\omega X = \sum_{i=1}^k \langle E_i, \nabla_{E_i} X \rangle,$$

where  $E_i$  is an orthonormal basis for  $\omega$  and  $\nabla$  is the Euclidean derivative. In particular, the equation (1.25) makes sense when  $\Sigma$  is a varifold and we will say that a varifold satisfying (1.25) is *stationary*.

As a consequence of (1.25), we have the following proposition:

**Proposition 1.1.**  *$\Sigma^k \subset \mathbf{R}^n$  is minimal if and only if the restrictions of the coordinate functions of  $\mathbf{R}^n$  to  $\Sigma$  are harmonic functions.*

*Proof.* Let  $\eta$  be a smooth function on  $\Sigma$  with compact support and  $\eta|_{\partial\Sigma} = 0$ , then

$$(1.27) \quad \int_\Sigma \langle \nabla_\Sigma \eta, \nabla_\Sigma x_i \rangle = \int_\Sigma \langle \nabla_\Sigma \eta, e_i \rangle = \int_\Sigma \operatorname{div}_\Sigma(\eta e_i).$$

From this, the claim follows easily.  $\square$

Recall that if  $\Xi \subset \mathbf{R}^n$  is a compact subset, then the smallest convex set containing  $\Xi$  (the convex hull,  $\operatorname{Conv}(\Xi)$ ) is the intersection of all half-spaces containing  $\Xi$ . The maximum principle forces a compact minimal submanifold to lie in the convex hull of its boundary (this is the ‘‘convex hull property’’):

**Proposition 1.2.** *If  $\Sigma^k \subset \mathbf{R}^n$  is a compact minimal submanifold, then  $\Sigma \subset \operatorname{Conv}(\partial\Sigma)$ .*

*Proof.* A half-space  $H \subset \mathbf{R}^n$  can be written as

$$(1.28) \quad H = \{x \in \mathbf{R}^n \mid \langle x, e \rangle \leq a\},$$

for a vector  $e \in \mathbf{S}^{n-1}$  and constant  $a \in \mathbf{R}$ . By Proposition 1.1, the function  $u(x) = \langle e, x \rangle$  is harmonic on  $\Sigma$  and hence attains its maximum on  $\partial\Sigma$  by the maximum principle.  $\square$

Another application of (1.24), with a different choice of vector field  $X$ , gives that for a  $k$ -dimensional minimal submanifold  $\Sigma$

$$(1.29) \quad \Delta_\Sigma |x - x_0|^2 = 2 \operatorname{div}_\Sigma(x - x_0) = 2k.$$

Later we will see that this formula plays a crucial role in the monotonicity formula for minimal submanifolds.

The argument in the proof of the convex hull property can be rephrased as saying that as we translate a hyperplane towards a minimal surface, the first point of contact must be on the boundary. When  $\Sigma$  is a hypersurface, this is a special case of the strong maximum principle for minimal surfaces (see [14] for a proof):

**Lemma 1.3.** *Let  $\Omega \subset \mathbf{R}^{n-1}$  be an open connected neighborhood of the origin. If  $u_1, u_2 : \Omega \rightarrow \mathbf{R}$  are solutions of the minimal surface equation with  $u_1 \leq u_2$  and  $u_1(0) = u_2(0)$ , then  $u_1 \equiv u_2$ .*

Since any smooth hypersurface is locally a graph over a hyperplane, Lemma 1.3 gives a maximum principle for smooth minimal hypersurfaces. There have been several interesting extensions of the maximum principle to the singular case.

For example, L. Simon, [97], proved that the strong maximum holds when both hypersurfaces are area-minimizing even in the presence of singularities. B. Solomon and B. White, [100], showed that it holds when at least one of the hypersurfaces is smooth (the other may be just a stationary varifold). Finally, T. Ilmanen, [48], showed that it holds for stationary hypersurfaces as long as each singular set has zero codimension two measure.

Thus far, the examples of minimal submanifolds have all been smooth. The simplest non-smooth example is given by a pair of planes intersecting transversely along a line. To get an example that is not even immersed, one can take three half-planes meeting along a line with an angle of  $2\pi/3$  between each adjacent pair.

## 2. MONOTONICITY AND THE MEAN VALUE INEQUALITY

Monotonicity formulas and mean value inequalities play a fundamental role in many areas of geometric analysis. Before we state and prove the monotonicity formula of volume for minimal submanifolds, we will need to recall the coarea formula. This formula asserts (see, for instance, [34] for a proof) that if  $\Sigma$  is a manifold and  $h : \Sigma \rightarrow \mathbf{R}$  is a Lipschitz function on  $\Sigma$ , then for all locally integrable functions  $f$  on  $\Sigma$  and  $t \in \mathbf{R}$

$$(2.1) \quad \int_{\{h \leq t\}} f |\nabla h| = \int_{-\infty}^t \int_{h=\tau} f d\tau.$$

When we apply this formula below,  $h$  will be Euclidean distance to a fixed point  $x_0$ .

**Proposition 2.1.** *Suppose that  $\Sigma^k \subset \mathbf{R}^n$  is a minimal submanifold and  $x_0 \in \mathbf{R}^n$ ; then for all  $0 < s < t$*

$$(2.2) \quad t^{-k} \text{Vol}(B_t(x_0) \cap \Sigma) - s^{-k} \text{Vol}(B_s(x_0) \cap \Sigma) = \int_{(B_t(x_0) \setminus B_s(x_0)) \cap \Sigma} \frac{|(x - x_0)^N|^2}{|x - x_0|^{k+2}}.$$

*Proof.* Within this proof, we set  $B_t = B_t(x_0)$ . Since  $\Sigma$  is minimal,

$$(2.3) \quad \Delta_\Sigma |x - x_0|^2 = 2 \text{div}_\Sigma(x - x_0) = 2k.$$

By Stokes' theorem integrating this gives

$$(2.4) \quad 2k \text{Vol}(B_s \cap \Sigma) = \int_{B_s \cap \Sigma} \Delta_\Sigma |x - x_0|^2 = 2 \int_{\partial B_s \cap \Sigma} |(x - x_0)^T|.$$

Using this and the coarea formula (i.e., (2.1)), an easy calculation gives

$$(2.5) \quad \begin{aligned} \frac{d}{ds} (s^{-k} \text{Vol}(B_s \cap \Sigma)) &= -k s^{-k-1} \text{Vol}(B_s \cap \Sigma) + s^{-k} \int_{\partial B_s \cap \Sigma} \frac{|x - x_0|}{|(x - x_0)^T|} \\ &= s^{-k-1} \int_{\partial B_s \cap \Sigma} \left( \frac{|x - x_0|^2}{|(x - x_0)^T|} - |(x - x_0)^T| \right) \\ &= s^{-k-1} \int_{\partial B_s \cap \Sigma} \frac{|(x - x_0)^N|^2}{|(x - x_0)^T|}. \end{aligned}$$

Integrating and applying the coarea formula once more gives the claim.  $\square$

Notice that  $(x - x_0)^N$  vanishes precisely when  $\Sigma$  is conical about  $x_0$ , i.e., when  $\Sigma$  is invariant under dilations about  $x_0$ . As a corollary, we get the following:

**Corollary 2.2.** *Suppose that  $\Sigma^k \subset \mathbf{R}^n$  is a minimal submanifold and  $x_0 \in \mathbf{R}^n$ ; then the function*

$$(2.6) \quad \Theta_{x_0}(s) = \frac{\text{Vol}(B_s(x_0) \cap \Sigma)}{\text{Vol}(B_s \subset \mathbf{R}^k)}$$

*is a nondecreasing function of  $s$ . Moreover,  $\Theta_{x_0}(s)$  is constant in  $s$  if and only if  $\Sigma$  is conical about  $x_0$ .*

Of course, if  $x_0$  is a smooth point of  $\Sigma$ , then  $\lim_{s \rightarrow 0} \Theta_{x_0}(s) = 1$ . We will later see that the converse is also true; this will be a consequence of the Allard regularity theorem.

The monotonicity of area is a very useful tool in the regularity theory for minimal surfaces — at least when there is some *a priori* area bound. For instance, this monotonicity and a compactness argument allow one to reduce many regularity questions to questions about minimal cones (this was a key observation of W. Fleming in his work on the Bernstein problem; see Section 4). Similar monotonicity formulas have played key roles in other geometric problems, including harmonic maps, Yang–Mills connections, J–holomorphic curves, and regularity of limit spaces with a lower Ricci curvature bound.

Arguing as in Proposition 2.1, we get a weighted monotonicity:

**Proposition 2.3.** *If  $\Sigma^k \subset \mathbf{R}^n$  is a minimal submanifold,  $x_0 \in \mathbf{R}^n$ , and  $f$  is a twice differentiable function on  $\Sigma$ , then*

$$(2.7) \quad t^{-k} \int_{B_t(x_0) \cap \Sigma} f - s^{-k} \int_{B_s(x_0) \cap \Sigma} f \\ = \int_{(B_t(x_0) \setminus B_s(x_0)) \cap \Sigma} f \frac{|(x - x_0)^N|^2}{|x - x_0|^{k+2}} + \frac{1}{2} \int_s^t \tau^{-k-1} \int_{B_\tau(x_0) \cap \Sigma} (\tau^2 - |x - x_0|^2) \Delta_\Sigma f \, d\tau.$$

We get immediately the following mean value inequality for the special case of non–negative subharmonic functions:

**Corollary 2.4.** *Suppose that  $\Sigma^k \subset \mathbf{R}^n$  is a minimal submanifold,  $x_0 \in \mathbf{R}^n$ , and  $f$  is a non–negative subharmonic function on  $\Sigma$ ; then*

$$(2.8) \quad s^{-k} \int_{B_s(x_0) \cap \Sigma} f$$

*is a nondecreasing function of  $s$ . In particular, if  $x_0 \in \Sigma$ , then for all  $s > 0$*

$$(2.9) \quad f(x_0) \leq \frac{\int_{B_s(x_0) \cap \Sigma} f}{\text{Vol}(B_s \subset \mathbf{R}^k)}.$$

### 3. RADO'S THEOREM

One of the most basic questions is what does the boundary  $\partial\Sigma$  tell us about a compact minimal submanifold  $\Sigma$ ? We have already seen that  $\Sigma$  must lie in the convex hull of  $\partial\Sigma$ , but there are many other theorems of this nature. One of the first is a beautiful result of T. Rado which says that if  $\partial\Sigma$  is a graph over the boundary of a convex set in  $\mathbf{R}^2$ , then  $\Sigma$  is also graph (and hence embedded). The proof of this uses basic properties of nodal lines for harmonic functions.



**Theorem 3.1.** *Suppose that  $\Omega \subset \mathbf{R}^2$  is a convex subset and  $\sigma \subset \mathbf{R}^3$  is a simple closed curve which is graphical over  $\partial\Omega$ . Then any minimal disk  $\Sigma \subset \mathbf{R}^3$  with  $\partial\Sigma = \sigma$  must be graphical over  $\Omega$  and hence unique by the maximum principle.*

*Proof.* (Sketch.) The proof is by contradiction, so suppose that  $\Sigma$  is such a minimal disk and  $x \in \Sigma$  is a point where the tangent plane to  $\Sigma$  is vertical. Consequently, there exists  $(a, b) \neq (0, 0)$  such that

$$(3.1) \quad \nabla_{\Sigma}(a x_1 + b x_2)(x) = 0.$$

By Proposition 1.1,  $a x_1 + b x_2$  is harmonic on  $\Sigma$  (since it is a linear combination of coordinate functions). The local structure of nodal sets of harmonic functions (see, e.g., [14]) then gives that the level set

$$(3.2) \quad \{y \in \Sigma \mid (a x_1 + b x_2)(y) = (a x_1 + b x_2)(x)\}$$

has a singularity at  $x$  where at least four different curves meet. If two of these nodal curves were to meet again, then there would be a closed nodal curve which must bound a disk (since  $\Sigma$  is a disk). By the maximum principle,  $a x_1 + b x_2$  would have to be constant on this disk and hence constant on  $\Sigma$  by unique continuation. This would imply that  $\sigma = \partial\Sigma$  is contained in the plane given by (3.2). Since this is impossible, we conclude that all of these curves go to the boundary without intersecting again.

In other words, the plane in  $\mathbf{R}^3$  given by (3.2) intersects  $\sigma$  in at least four points. However, since  $\Omega \subset \mathbf{R}^2$  is convex,  $\partial\Omega$  intersects the line given by (3.2) in exactly two points. Finally, since  $\sigma$  is graphical over  $\partial\Omega$ ,  $\sigma$  intersects the plane in  $\mathbf{R}^3$  given by (3.2) in exactly two points, which gives the desired contradiction.  $\square$

#### 4. THE THEOREMS OF BERNSTEIN AND BERS

A classical theorem of S. Bernstein from 1916 says that entire (i.e., defined over all of  $\mathbf{R}^2$ ) minimal graphs are planes. This remarkable theorem of Bernstein was one of the first illustrations of the fact that the solutions to a nonlinear PDE, like the minimal surface equation, can behave quite differently from solutions to a linear equation.

**Theorem 4.1.** [5] *If  $u : \mathbf{R}^2 \rightarrow \mathbf{R}$  is an entire solution to the minimal surface equation, then  $u$  is an affine function.*

*Proof.* (Sketch.) We will show that the curvature of the graph vanishes identically; this implies that the unit normal is constant and, hence, the graph must be a plane. The proof follows by combining two facts. First, the area estimate for graphs (1.21) gives

$$(4.1) \quad \text{Area}(B_r \cap \text{Graph}_u) \leq 2\pi r^2.$$

This quadratic area growth allows one to construct a sequence of non-negative logarithmic cutoff functions  $\phi_j$  defined on the graph with  $\phi_j \rightarrow 1$  everywhere and

$$(4.2) \quad \lim_{j \rightarrow \infty} \int_{\text{Graph}_u} |\nabla \phi_j|^2 = 0.$$

Moreover, since graphs are area-minimizing, they must be stable. We can therefore use  $\phi_j$  in the stability inequality (1.7) to get

$$(4.3) \quad \int_{\text{Graph}_u} \phi_j^2 |A|^2 \leq \int_{\text{Graph}_u} |\nabla \phi_j|^2.$$

Combining these gives that  $|A|^2$  is zero, as desired.  $\square$

Rather surprisingly, this result very much depended on the dimension. The combined efforts of E. De Giorgi [31], F. J. Almgren, Jr. [2], and J. Simons [98] finally gave:

**Theorem 4.2.** *If  $u : \mathbf{R}^{n-1} \rightarrow \mathbf{R}$  is an entire solution to the minimal surface equation and  $n \leq 8$ , then  $u$  is an affine function.*

However, in 1969 E. Bombieri, De Giorgi, and E. Giusti [8] constructed entire non-affine solutions to the minimal surface equation on  $\mathbf{R}^8$  and an area-minimizing singular cone in  $\mathbf{R}^8$ . In fact, they showed that for  $m \geq 4$  the cones

$$(4.4) \quad C_m = \{(x_1, \dots, x_{2m}) \mid x_1^2 + \dots + x_m^2 = x_{m+1}^2 + \dots + x_{2m}^2\} \subset \mathbf{R}^{2m}$$

are area-minimizing (and obviously singular at the origin).

In contrast to the entire case, exterior solutions of the minimal graph equation, i.e., solutions on  $\mathbf{R}^2 \setminus B_1$ , are much more plentiful. In this case, L. Bers proved that  $\nabla u$  actually has an asymptotic limit:

**Theorem 4.3.** [6] *If  $u$  is a  $C^2$  solution to the minimal surface equation on  $\mathbf{R}^2 \setminus B_1$ , then  $\nabla u$  has a limit at infinity (i.e., there is an asymptotic tangent plane).*

*Proof.* (Sketch.) To get a rough idea of why Bers' theorem should hold, recall that the Gauss map  $\mathbf{n}$  gives a holomorphic map from the graph of  $u$  to the upper hemisphere. Hence, composing  $\mathbf{n}$  with stereographic projection gives a bounded holomorphic function on the graph of  $u$ .

The rest of the argument is to show that the point at infinity is a removable singularity for this bounded holomorphic function. Since the graph of  $u$  is a topological annulus, it must be conformal to an annulus of the form  $\{a < |z| \leq 1\}$  in the plane for some  $a \geq 0$ . The point is to show that  $a = 0$ . Arguing as in the proof of Bernstein's theorem (cf. (4.1)) shows that the graph of  $u$  has quadratic area growth and, hence, we can construct logarithmic cutoff functions "at infinity" with arbitrarily small energy. It follows that we must have  $a = 0$  and hence  $\mathbf{n}$  extends smoothly across the puncture. This gives a limiting value for  $\mathbf{n}$  and, consequently, also a limiting value for  $\nabla u$ .  $\square$

Bers' theorem was extended to higher dimensions by L. Simon:

**Theorem 4.4.** [94] *If  $u$  is a  $C^2$  solution to the minimal surface equation on  $\mathbf{R}^n \setminus B_1$ , then either*

- $|\nabla u|$  is bounded and  $\nabla u$  has a limit at infinity.
- All tangent cones at infinity are of the form  $\Sigma \times \mathbf{R}$  where  $\Sigma$  is singular.

Bernstein's theorem has had many other interesting generalizations, some of which will be discussed later.

## 5. SIMONS INEQUALITY

In this section, we recall a very useful differential inequality for the Laplacian of the norm squared of the second fundamental form  $A$  of a minimal hypersurface  $\Sigma$  in  $\mathbf{R}^n$  and illustrate its role in *a priori* estimates. This inequality, originally due to J. Simons (see [14] for a proof and further discussion), is:

**Lemma 5.1.** [98] *If  $\Sigma^{n-1} \subset \mathbf{R}^n$  is a minimal hypersurface, then*

$$(5.1) \quad \Delta_{\Sigma} |A|^2 = -2|A|^4 + 2|\nabla_{\Sigma} A|^2 \geq -2|A|^4.$$

An inequality of the type (5.1) on its own does not lead to pointwise bounds on  $|A|^2$  because of the nonlinearity. However, it does lead to estimates if a “scale-invariant energy” is small. For example, H. Choi and R. Schoen used (5.1) to prove:

**Theorem 5.2.** [12] *There exists  $\epsilon > 0$  so that if  $0 \in \Sigma \subset B_r(0)$  with  $\partial\Sigma \subset \partial B_r(0)$  is a minimal surface with*

$$(5.2) \quad \int |A|^2 \leq \epsilon,$$

*then*

$$(5.3) \quad |A|^2(0) \leq r^{-2}.$$

## 6. HEINZ’S CURVATURE ESTIMATE FOR GRAPHS

One of the key themes in minimal surface theory is the usefulness of *a priori* estimates. A basic example is the curvature estimate of E. Heinz for minimal graphs over a disk  $D_{r_0}$  of radius  $r_0$  in the plane.

**Theorem 6.1.** [41] *If  $D_{r_0} \subset \mathbf{R}^2$  and  $u : D_{r_0} \rightarrow \mathbf{R}$  satisfies the minimal surface equation, then for  $\Sigma = \text{Graph}_u$  and  $0 < \sigma \leq r_0$*

$$(6.1) \quad \sigma^2 \sup_{D_{r_0-\sigma}} |A|^2 \leq C.$$

*Proof.* (Sketch.) Observe first that it suffices to prove the estimate for  $\sigma = r_0$ , i.e., to show that

$$(6.2) \quad |A|^2(0, u(0)) \leq C r_0^{-2}.$$

Recall that minimal graphs are automatically stable. As in the proof of Theorem 4.1, the area estimate for graphs (1.21) allows us to use a logarithmic cutoff function in the the stability inequality (1.7) to get that

$$(6.3) \quad \int_{B_{r_1} \cap \text{Graph}_u} |A|^2 \leq \frac{C}{\log(r_0/r_1)}.$$

Taking  $r_0/r_1$  sufficiently large, we can then apply Theorem 5.2 to get (6.2).  $\square$

Heinz’s estimate gives an effective version of the Bernstein’s theorem; namely, letting the radius  $r_0$  go to infinity in (6.1) implies that  $|A|$  vanishes, thus giving Bernstein’s theorem.

## 7. EMBEDDED MINIMAL DISKS WITH AREA BOUNDS

In the early nineteen-eighties R. Schoen and L. Simon extended the theorem of Bernstein to complete simply connected embedded minimal surfaces in  $\mathbf{R}^3$  with quadratic area growth; see [90]. A surface  $\Sigma$  is said to have *quadratic area growth* if for all  $r > 0$ , the area of the intersection of the surface with the ball in  $\mathbf{R}^3$  of radius  $r$  and center at the origin is bounded by  $C r^2$  for a fixed constant  $C$  independent of  $r$ .

**Theorem 7.1.** [90] *Let  $0 \in \Sigma^2 \subset B_{r_0} = B_{r_0}(x) \subset \mathbf{R}^3$  be an embedded simply connected minimal surface with  $\partial\Sigma \subset \partial B_{r_0}$ . If  $\mu > 0$  and either*

$$(7.1) \quad \text{Area}(\Sigma) \leq \mu r_0^2, \text{ or}$$

$$(7.2) \quad \int_{\Sigma} |A|^2 \leq \mu,$$

*then for the connected component  $\Sigma'$  of  $B_{r_0/2}(x_0) \cap \Sigma$  with  $0 \in \Sigma'$  we have*

$$(7.3) \quad \sup_{\Sigma'} |A|^2 \leq C r_0^{-2}$$

*for some  $C = C(\mu)$ .*

In corollary 1.18 in [17], this was generalized to quadratic area growth for *intrinsic* balls (this generalization played an important role in analyzing the local structure of embedded minimal surfaces). We will use  $\mathcal{B}_r(p)$  to denote the *intrinsic ball* of radius  $r$  centered at a point  $p$  in a surface  $\Sigma$ , i.e.,  $\mathcal{B}_r(p)$  is the set of points  $q$  in  $\Sigma$  that can be connected to  $p$  by a path  $\gamma$  in  $\Sigma$  of length less than  $r$ .

**Theorem 7.2.** [17] *Given a constant  $C_I$ , there exists  $C_P$  so that if  $\mathcal{B}_{2r_0} \subset \Sigma \subset \mathbf{R}^3$  is an embedded minimal disk satisfying either*

$$(7.4) \quad \text{Area}(\mathcal{B}_{2r_0}) \leq C_I r_0^2 \text{ or}$$

$$(7.5) \quad \int_{\mathcal{B}_{2r_0}} |A|^2 \leq C_I,$$

*then*

$$(7.6) \quad \sup_{B_s} |A|^2 \leq C_P s^{-2}.$$

As an immediate consequence, letting  $r_0 \rightarrow \infty$  gives Bernstein-type theorems for embedded simply connected minimal surfaces with either bounded density or finite total curvature.

The classical minimal surfaces known as Enneper's surface and the catenoid show that neither "embedded" nor "simply-connected" can be removed. Enneper's surface is a complete immersed minimal disk but is not flat and is not embedded (see (17.3) for the definition of Enneper's surface). This example shows that embeddedness is essential for these estimates. Similarly, the catenoid shows that simply-connected is essential. The catenoid is the minimal surface in  $\mathbf{R}^3$  given by

$$(7.7) \quad \{(\cosh s \cos t, \cosh s \sin t, s) \mid s, t \in \mathbf{R}\};$$

see figure 5.

## 8. STABLE MINIMAL SURFACES

It turns out that stable minimal surfaces have *a priori* estimates. Since minimal graphs are stable, the estimates for stable surfaces can be thought of as generalizations of the earlier estimates for graphs. These estimates have been widely applied and are particularly useful when combined with existence results for stable surfaces (such as the solution of the Plateau problem). The starting point for these estimates is that, as we saw in (1.4), stable minimal surfaces satisfy the stability inequality

$$(8.1) \quad \int |A|^2 \phi^2 \leq \int |\nabla \phi|^2.$$

We will mention two such estimates. The first is R. Schoen's curvature estimate for stable surfaces:

**Theorem 8.1.** [88] *There exists a constant  $C$  so that if  $\Sigma \subset \mathbf{R}^3$  is an immersed stable minimal surface with trivial normal bundle and  $\mathcal{B}_{r_0} \subset \Sigma \setminus \partial\Sigma$ , then*

$$(8.2) \quad \sup_{\mathcal{B}_{r_0-\sigma}} |A|^2 \leq C \sigma^{-2}.$$

The second is an estimate for the area and total curvature of a stable surface; for simplicity, we will state only the area estimate:

**Theorem 8.2.** [15] *If  $\Sigma \subset \mathbf{R}^3$  is an immersed stable minimal surface with trivial normal bundle and  $\mathcal{B}_{r_0} \subset \Sigma \setminus \partial\Sigma$ , then*

$$(8.3) \quad \text{Area}(\mathcal{B}_{r_0}) \leq 4\pi r_0^2/3.$$

As mentioned, we can use (8.3) to bound the energy of a cutoff function in the stability inequality and, thus, bound the total curvature of sub-balls. Combining this with the curvature estimate of Theorem 5.2 gives Theorem 8.1; see [15]. Note that the bound (8.3) is surprisingly sharp; even when  $\Sigma$  is a plane, the area is  $\pi r_0^2$ .

We will explain next why Theorem 8.2 holds. The stability inequality can be used to get upper bounds for the total curvature in terms of the area of a minimal surface. On the other hand, we can use either the Gauss–Bonnet theorem or the Jacobi equation to get the opposite bound. Combining these two bounds will give the *a priori* bound on the area of intrinsic balls in a stable surface. More precisely, integrating the Jacobi equation and using the Gauss equation  $K_\Sigma = -|A|^2/2$  gives

$$(8.4) \quad 4(\text{Area}(\mathcal{B}_R) - \pi R^2) = 2 \int_0^R \int_0^t \int_{\mathcal{B}_s} |A|^2 = \int_{\mathcal{B}_R} |A|^2 (R-r)^2.$$

The second equality uses two integrations by parts (i.e.,  $\int_0^R f(t) g''(t) dt$  with  $f(t) = \int_0^t \int_{\mathcal{B}_s} |A|^2$  and  $g(t) = (R-t)^2$ ). See corollary 1.7 of [17] for further details.

Using  $\phi = R-r$  (where  $r(x) = \text{dist}_\Sigma(0, x)$ ) in the stability inequality gives

$$(8.5) \quad 4(\text{Area}(\mathcal{B}_R) - \pi R^2) = \int_{\mathcal{B}_R} |A|^2 (R-r)^2 \leq \int_{\mathcal{B}_R} |\nabla(R-r)|^2 = \text{Area}(\mathcal{B}_R).$$

Consequently,  $\text{Area}(\mathcal{B}_R) \leq 4\pi R^2/3$ .

## 9. REGULARITY THEORY

In this section, we survey some of the key ideas in classical regularity theory, such as the role of monotonicity, scaling,  $\epsilon$ -regularity theorems (such as W. Allard's theorem) and tangent cone analysis (such as F. Almgren's refinement of H. Federer's dimension reducing).

The starting point for all of this is the monotonicity of volume for a minimal  $k$ -dimensional submanifold  $\Sigma$ . Namely, Corollary 2.2 gives that the *density*

$$(9.1) \quad \Theta_{x_0}(s) = \frac{\text{Vol}(B_s(x_0) \cap \Sigma)}{\text{Vol}(B_s \subset \mathbf{R}^k)}$$

is a monotone non-decreasing function of  $s$ . Consequently, we can define the density  $\Theta_{x_0}$  at the point  $x_0$  to be the limit as  $s \rightarrow 0$  of  $\Theta_{x_0}(s)$ . It also follows easily from monotonicity that the density is semi-continuous as a function of  $x_0$ .

**9.1.  $\epsilon$ -regularity and the singular set.** An  $\epsilon$ -regularity theorem is a theorem giving that a weak (or generalized) solution is actually smooth at a point if a scale-invariant energy is small enough there. The standard example is the Allard regularity theorem:

**Theorem 9.1.** [1] *There exists  $\delta = \delta(k, n) > 0$  such that if  $\Sigma \subset \mathbf{R}^n$  is a  $k$ -rectifiable stationary varifold (with density at least one a.e.),  $x_0 \in \Sigma$ , and*

$$(9.2) \quad \Theta_{x_0} = \lim_{r \rightarrow 0} \frac{\text{Vol}(B_r(x_0) \cap \Sigma)}{\text{Vol}(B_r \subset \mathbf{R}^k)} < 1 + \delta,$$

then  $\Sigma$  is smooth in a neighborhood of  $x_0$ .

Similarly, the small total curvature estimate of Theorem 5.2 may be thought of as an  $\epsilon$ -regularity theorem; in this case, the scale-invariant energy is  $\int |A|^2$ .

As an application of the  $\epsilon$ -regularity theorem, Theorem 9.1, we can define the singular set  $\mathcal{S}$  of  $\Sigma$  by

$$(9.3) \quad \mathcal{S} = \{x \in \Sigma \mid \Theta_x \geq 1 + \delta\}.$$

It follows immediately from the semi-continuity of the density that  $\mathcal{S}$  is closed. In order to bound the size of the singular set (e.g., the Hausdorff measure), one combines the  $\epsilon$ -regularity with simple covering arguments.

This preliminary analysis of the singular set can be refined by doing a so-called tangent cone analysis.

**9.2. Tangent cone analysis.** It is not hard to see that scaling preserves the space of minimal submanifolds of  $\mathbf{R}^n$ . Namely, if  $\Sigma$  is minimal, then so is

$$(9.4) \quad \Sigma_{y,\lambda} = \{y + \lambda^{-1}(x - y) \mid x \in \Sigma\}.$$

(To see this, simply note that this scaling multiplies the principal curvatures by  $\lambda$ .) Suppose now that we fix the point  $y$  and take a sequence  $\lambda_j \rightarrow 0$ . The monotonicity formula bounds the density of the rescaled solution, allowing us to extract a convergent subsequence and limit. This limit, which is called a *tangent cone* at  $y$ , achieves equality in the monotonicity formula and, hence, must be homogeneous (i.e., invariant under dilations about  $y$ ).

The usefulness of tangent cone analysis in regularity theory is based on two key facts. For simplicity, we illustrate these when  $\Sigma \subset \mathbf{R}^n$  is an area minimizing hypersurface. First, if any tangent cone at  $y$  is a hyperplane  $\mathbf{R}^{n-1}$ , then  $\Sigma$  is smooth in a neighborhood of  $y$ . This follows easily from the Allard regularity theorem since the density at  $y$  of the tangent cone is the same as the density at  $y$  of  $\Sigma$ . The second key fact, known as “dimension reducing,” is due to F. Almgren, [3], and is a refinement of an argument of H. Federer. To state this, we first stratify the singular set  $\mathcal{S}$  of  $\Sigma$  into subsets

$$(9.5) \quad \mathcal{S}_0 \subset \mathcal{S}_1 \subset \cdots \subset \mathcal{S}_{n-2},$$

where we define  $\mathcal{S}_i$  to be the set of points  $y \in \mathcal{S}$  so that any linear space contained in any tangent cone at  $y$  has dimension at most  $i$ . (Note that  $\mathcal{S}_{n-1} = \emptyset$  by Allard’s Theorem.) The dimension reducing argument then gives that

$$(9.6) \quad \dim(\mathcal{S}_i) \leq i,$$

where dimension means the Hausdorff dimension. In particular, the solution of the Bernstein problem then gives codimension 7 regularity of  $\Sigma$ , i.e.,  $\dim(\mathcal{S}) \leq n - 8$ . See lecture 2 in [96] for a proof of (9.6).

Tangent cones produced by scalings as above may very well depend on the particular convergent subsequence. In some cases, one can prove uniqueness of the tangent cone and this is often quite useful (see, for instance, section 3.4 in [96] for one such application).

## Part 2. Embedded minimal surfaces

Thus far, the results for embedded minimal surfaces have assumed some additional *a priori* bound, such as bounds on area or total curvature, and the proofs break down without these *a priori* bounds. In this part, we will focus on recent results for embedded minimal surfaces without *a priori* bounds.

**10.1. Multi-valued graphs.** We have earlier studied minimal graphs. It is useful also to consider multi-valued minimal graphs. Intuitively, an (embedded) multi-valued graph is a surface such that over each point of the annulus, the surface consists of  $N$  graphs. To make this notion precise, let  $\mathcal{P}$  be the universal cover of the punctured plane  $\mathbf{C} \setminus \{0\}$  with global polar coordinates  $(\rho, \theta)$  so  $\rho > 0$  and  $\theta \in \mathbf{R}$ . An  $N$ -valued graph on  $\mathbf{C} \setminus \{0\}$  is a single valued graph of a function  $u$  over  $\mathcal{P}$ . For working purposes, we generally think of the intuitive picture of a multi-sheeted surface in  $\mathbf{R}^3$ , and we identify the single-valued graph over the universal cover with its multi-valued image in  $\mathbf{R}^3$ .

We will also need the notion of an  $N$ -valued graph over the annulus  $\{r < \rho \leq s\} \subset \mathbf{C}$ . In this case, the function is single-valued on

$$(10.1) \quad \{(\rho, \theta) \mid r < \rho \leq s, |\theta| \leq N\pi\}.$$

The multi-valued graphs that we will consider will all be embedded, which corresponds to a nonvanishing separation between the sheets (or the floors). Here the *separation* is the function (see figure 2)

$$(10.2) \quad w(\rho, \theta) = u(\rho, \theta + 2\pi) - u(\rho, \theta).$$

The helicoid is a minimal surface consisting of two multi-valued graphs glued together along an axis. The helicoid looks like a “double spiral staircase” (see [23]) and is parametrized by:

**Example 2:** (Helicoid; see figure 1). The helicoid is the minimal surface in  $\mathbf{R}^3$  given by the parametrization

$$(10.3) \quad (s \cos t, s \sin t, t), \quad \text{where } s, t \in \mathbf{R}.$$

If  $\Sigma$  is the helicoid, then  $\Sigma \setminus \{x_3 - \text{axis}\} = \Sigma_1 \cup \Sigma_2$ , where  $\Sigma_1, \Sigma_2$  are  $\infty$ -valued graphs on  $\mathbf{C} \setminus \{0\}$ .  $\Sigma_1$  is the graph of the function  $u_1(\rho, \theta) = \theta$  and  $\Sigma_2$  is the graph of the function  $u_2(\rho, \theta) = \theta + \pi$ . ( $\Sigma_1$  is the subset where  $s > 0$  in (10.3) and  $\Sigma_2$  the subset where  $s < 0$ .) In either case the separation  $w = 2\pi$ . A *multi-valued minimal graph* is a multi-valued graph of a function  $u$  satisfying the minimal surface equation.

Note that for an embedded multi-valued graph, the sign of  $w$  determines whether the multi-valued graph spirals in a left-handed or right-handed manner, in other

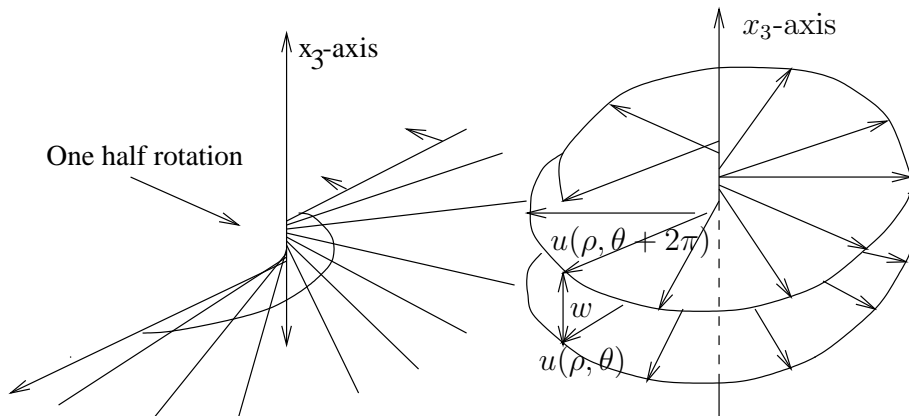


FIGURE 1. Multi-valued graphs. The helicoid is obtained by gluing together two  $\infty$ -valued graphs along a line. First published in the Notices of the American Mathematical Society in 2003, published by the American Mathematical Society.

FIGURE 2. The separation  $w$  grows/decays in  $\rho$  at most sublinearly for a multi-valued minimal graph; see (10.5).

words, whether upwards motion corresponds to turning in a clockwise direction or in a counterclockwise direction.

**10.2. The sublinear growth of the separation.** As we have seen, the separation is constant for the multi-valued graphs coming from each half of the helicoid. This can be viewed as a type of Liouville Theorem reflecting the conformal properties of an infinite-valued graph. In Proposition II.2.12 of [16], we proved a corresponding gradient estimate (i.e., a pointwise estimate for  $|\nabla \log |w||$ ) for a general multi-valued graph. Integrating this gradient estimate gives that the separation grows sublinearly (see figure 2):

**Proposition 10.1.** [16] *Given  $\alpha > 0$ , there exists  $N$  so that if  $u$  satisfies the minimal surface equation on*

$$(10.4) \quad \{e^{-N} r_1 \leq \rho \leq e^N r_2, -N \leq \theta \leq 2\pi + N\},$$

*$|\nabla u| \leq 1$ , and has separation  $w \neq 0$ , then*

$$(10.5) \quad |w|(r_2, 0) \leq |w|(r_1, 0) \left(\frac{r_2}{r_1}\right)^\alpha.$$

*Proof.* (Sketch.) As mentioned above, the inequality (10.5) follows from integrating the gradient estimate

$$(10.6) \quad |\nabla \log |w|| (r, 0) \leq \frac{\alpha}{r}$$

in the same way that the Harnack inequality for positive harmonic functions follows from integrating the gradient estimate.



To see why a gradient estimate like (10.6) holds, observe that  $u(\cdot, \cdot)$  and its  $2\pi$ -rotation  $u(\cdot, \cdot + 2\pi)$  are both solutions of the minimal surface equation and, thus, the difference  $w$  is (almost) a positive solution of the linearized equation. The linearized equation is itself a perturbation of the Laplace equation and it is not difficult to get an estimate

$$(10.7) \quad |\nabla \log |w|| (r, 0) \leq \frac{C}{r},$$

for some constant  $C$ .

The point now is to show that if  $N$  is large, then we can make the constant  $C$  in (10.7) small. For simplicity, suppose that  $w$  is actually a positive harmonic function on the region (10.4). Since harmonic functions are invariant under conformal transformations,  $w \circ e^z$  is a positive harmonic function on the “rectangle”

$$(10.8) \quad \{(x + iy) \mid -N + \log r_1 < x < N + \log r_2 \text{ and } |y| < N\}.$$

In the extreme case when  $N = \infty$ , the positive harmonic function  $w \circ e^z$  is defined on the entire plane and, hence, is constant by the Liouville theorem. It is not hard to see that applying the gradient estimate on this rectangle when  $N$  is large, and then translating this back to the original function  $w$ , gives (10.6).  $\square$

## 11. EMBEDDED MINIMAL DISKS

There are two classical local models for embedded minimal disks (by an *embedded disk* we mean a smooth injective map from the closed unit ball in  $\mathbf{R}^2$  into  $\mathbf{R}^3$ ). One model is the plane (or, more generally, a minimal graph) and the other is a piece of a helicoid.

The helicoid was discovered by Meusnier in 1776. Meusnier had been a student of Monge. He also discovered that the surface now known as the catenoid is minimal in the sense of Lagrange, and he was the first to characterize a minimal surface as a surface with vanishing mean curvature. Unlike the helicoid, the catenoid is not topologically a plane but rather a cylinder.

It turns out that these two classical examples (graphs and helicoids) completely capture the local structure of an embedded minimal disk. This is made concrete in the compactness theorem for embedded minimal disks, Theorem 11.1 below.

To avoid tedious dependence of various quantities we state Theorem 11.1 not for a single embedded minimal disk with sufficiently large curvature at a given point but instead for a sequence of such disks where the curvatures are blowing up. Theorem 11.1 says that a sequence of embedded minimal disks mimics the following behavior of a sequence of rescaled helicoids:

Consider the sequence  $\Sigma_i = a_i \Sigma$  of rescaled helicoids where  $a_i \rightarrow 0$ . (That is, rescale  $\mathbf{R}^3$  by  $a_i$ , so points that used to be distance  $d$  apart will in the rescaled  $\mathbf{R}^3$  be distance  $a_i d$  apart.) The curvatures of this sequence of rescaled helicoids are blowing up along the vertical axis. The sequence converges (away from the vertical axis) to a foliation by flat parallel planes. The singular set  $\mathcal{S}$  (the axis) then consists of removable singularities.

Let now  $\Sigma_i \subset B_{2R}$  be a sequence of embedded minimal disks with  $\partial \Sigma_i \subset \partial B_{2R}$ . Clearly (after possibly going to a subsequence) either (A) or (B) occurs:

(A)  $\sup_{B_R \cap \Sigma_i} |A|^2 \leq C < \infty$  for some constant  $C$ .

(B)  $\sup_{B_R \cap \Sigma_i} |A|^2 \rightarrow \infty$ .

In (A) (by a standard argument; see, e.g., lemma 2.2 in [14]) the intrinsic ball  $\mathcal{B}_s(y_i)$  is a graph for all  $y_i \in B_R \cap \Sigma_i$ , where  $s$  depends only on  $C$ . Thus the main case is (B) which is the subject of the next theorem.

Using the notion of multi-valued graphs, the *lamination theorem* (the main theorem of [19]), can now be stated:

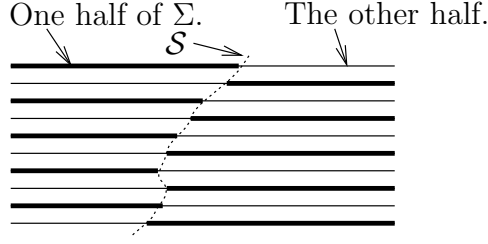


FIGURE 3. Theorem 11.1 – the singular set,  $\mathcal{S}$ , and the two multi-valued graphs. First published in the Notices of the American Mathematical Society in 2003, published by the American Mathematical Society.

**Theorem 11.1.** (*Theorem 0.1 in [19]*). *See figure 3. Let  $\Sigma_i \subset B_{R_i} = B_{R_i}(0) \subset \mathbf{R}^3$  be a sequence of embedded minimal disks with  $\partial\Sigma_i \subset \partial B_{R_i}$  where  $R_i \rightarrow \infty$ . If*

$$(11.1) \quad \sup_{B_1 \cap \Sigma_i} |A|^2 \rightarrow \infty,$$

*then there exists a subsequence,  $\Sigma_j$ , and a Lipschitz curve  $\mathcal{S} : \mathbf{R} \rightarrow \mathbf{R}^3$  such that after a rotation of  $\mathbf{R}^3$ :*

- (1)  $x_3(\mathcal{S}(t)) = t$ . (*That is,  $\mathcal{S}$  is a graph over the  $x_3$ -axis.*)
- (2) *Each  $\Sigma_j$  consists of exactly two multi-valued graphs away from  $\mathcal{S}$  (which spiral together).*
- (3) *For each  $1 > \alpha > 0$ ,  $\Sigma_j \setminus \mathcal{S}$  converges in the  $C^\alpha$ -topology to the foliation,  $\mathcal{F} = \{x_3 = t\}_t$ , of  $\mathbf{R}^3$ .*
- (4)  $\sup_{B_r(\mathcal{S}(t)) \cap \Sigma_j} |A|^2 \rightarrow \infty$  for all  $r > 0$ ,  $t \in \mathbf{R}$ . (*The curvatures blow up along  $\mathcal{S}$ .*)

In (2) and (3), the statements that  $\Sigma_j \setminus \mathcal{S}$  are multi-valued graphs and converges to  $\mathcal{F}$  means that for each compact subset  $K \subset \mathbf{R}^3 \setminus \mathcal{S}$  and  $j$  sufficiently large  $K \cap \Sigma_j$  consists of multi-valued graphs over (part of)  $\{x_3 = 0\}$  and  $K \cap \Sigma_j \rightarrow K \cap \mathcal{F}$  in the sense of graphs.

A key point in Theorem 11.1 is that there is no useful monotonicity formula or natural *a priori* bound. The main tools for overcoming these difficulties are a “classification of singularities” which describes a neighborhood of points of large curvature and our one-sided curvature estimate (Theorem 11.2 below).

The one-sided curvature estimate says roughly that if an embedded minimal disk lies in a half-space above a plane and comes close to the plane, then it is a graph over the plane. Precisely, this is the following theorem:

**Theorem 11.2.** (*Theorem 0.2 in [19]*). *See figure 4. There exists  $\epsilon > 0$ , so that if*

$$\Sigma \subset B_{2r_0} \cap \{x_3 > 0\} \subset \mathbf{R}^3$$

is an embedded minimal disk with  $\partial\Sigma \subset \partial B_{2r_0}$ , then for all components  $\Sigma'$  of  $B_{r_0} \cap \Sigma$  which intersect  $B_{\epsilon r_0}$  we have

$$(11.2) \quad \sup_{\Sigma'} |A_\Sigma|^2 \leq r_0^{-2}.$$

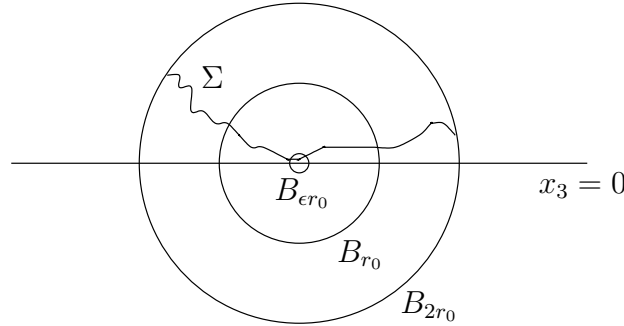


FIGURE 4. Theorem 11.2 – the one-sided curvature estimate for an embedded minimal disk  $\Sigma$  in a half-space with  $\partial\Sigma \subset \partial B_{2r_0}$ : The components of  $B_{r_0} \cap \Sigma$  intersecting  $B_{\epsilon r_0}$  are graphs. First published in the Notices of the American Mathematical Society in 2003, published by the American Mathematical Society.

Using the minimal surface equation and that  $\Sigma'$  has points close to a plane, it is not hard to see that, for  $\epsilon > 0$  sufficiently small, (11.2) is equivalent to the statement that  $\Sigma'$  is a graph over the plane  $\{x_3 = 0\}$ .

We will often refer to Theorem 11.2 as *the one-sided curvature estimate*.

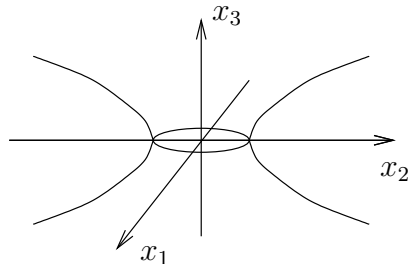


FIGURE 5. The catenoid given by revolving  $x_1 = \cosh x_3$  around the  $x_3$ -axis. First published in the Notices of the American Mathematical Society in 2003, published by the American Mathematical Society.

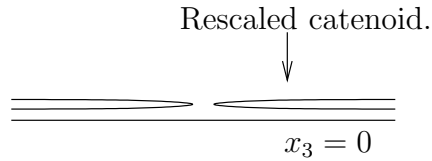


FIGURE 6. Rescaling the catenoid shows that simply connected (and embedded) is needed in the one-sided curvature estimate. First published in the Notices of the American Mathematical Society in 2003, published by the American Mathematical Society.

Note that the assumption in Theorem 11.2 that  $\Sigma$  is simply connected is crucial as can be seen from the example of a rescaled catenoid. Recall that the catenoid is the minimal surface in  $\mathbf{R}^3$  given by

$$(11.3) \quad (\cosh s \cos t, \cosh s \sin t, s)$$

where  $s, t \in \mathbf{R}$ ; see figure 5. Under rescalings this converges (with multiplicity two) to the flat plane; see figure 6. Likewise, by considering the universal cover of the catenoid, one sees that embedded, and not just immersed, is needed in Theorem 11.2.

As an almost immediate consequence of Theorem 11.2 and a simple barrier argument we get that if in a ball two embedded minimal disks come close to each other near the center of the ball then each of the disks are graphs. Precisely, this is the following:

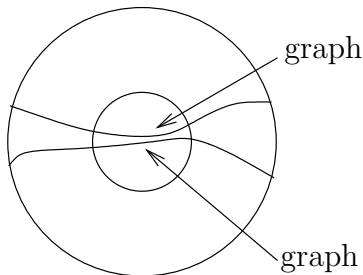


FIGURE 7. Corollary 11.3: Two sufficiently close components of an embedded minimal disk must each be a graph.

**Corollary 11.3.** (*Corollary 0.4 in [19]*). *See figure 7. There exist  $c > 1$ ,  $\epsilon > 0$  so that the following holds:*

*Let  $\Sigma_1$  and  $\Sigma_2 \subset B_{cr_0} \subset \mathbf{R}^3$  be disjoint embedded minimal surfaces with  $\partial\Sigma_i \subset \partial B_{cr_0}$  and  $B_{\epsilon r_0} \cap \Sigma_i \neq \emptyset$ . If  $\Sigma_1$  is a disk, then for all components  $\Sigma'_1$  of  $B_{r_0} \cap \Sigma_1$  which intersect  $B_{\epsilon r_0}$*

$$(11.4) \quad \sup_{\Sigma'_1} |A|^2 \leq r_0^{-2}.$$

## 12. FIXED GENUS

Following our results on embedded minimal disks described in the previous section, we proved two main structure theorems for *non-simply connected* embedded minimal surfaces of any given fixed genus in [20].

The first of these asserts that any such surface without small necks can be obtained by gluing together two oppositely-oriented double spiral staircases; see figure 8.

The second gives a pair of pants decomposition of any such surface when there are small necks, cutting the surface along a collection of short curves; see figure 9. After the cutting, we are left with graphical pieces that are defined over a disk with either one or two sub-disks removed (a topological disk with two sub-disks removed is called a pair of pants).

Both of these structures occur as different extremes in the two-parameter family of minimal surfaces known as the Riemann examples.

**12.1. Uniformly locally simply connected.** Sequences of surfaces which are not simply connected are, after passing to a subsequence, naturally divided into two separate cases depending on whether or not the topology is concentrating at points. To distinguish between these cases, we will say that a sequence of surfaces

The two main structure theorems for non-simply connected surfaces:

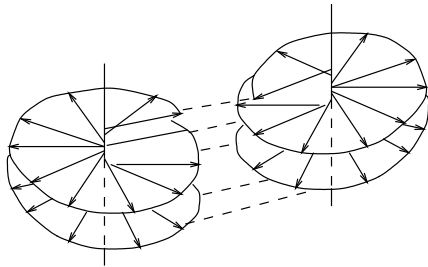
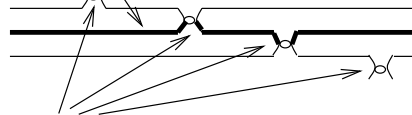


FIGURE 8. Absence of necks: The surface can be obtained by gluing together two oppositely-oriented double spiral staircases.

One of the “pair of pants” (in bold).



The curves that we cut along.

FIGURE 9. Presence of necks: The surface can be decomposed into a collection of pair of pants by cutting along short curves.

$\Sigma_i^2 \subset \mathbf{R}^3$  is *uniformly locally simply connected* (or ULSC) if for each compact subset  $K$  of  $\mathbf{R}^3$ , there exists a constant  $r_0 > 0$  (depending on  $K$ ) so that for every  $x \in K$ , all  $r \leq r_0$ , and every surface  $\Sigma_i$

$$(12.1) \quad \text{each connected component of } B_r(x) \cap \Sigma_i \text{ is a disk.}$$

For instance, a sequence of rescaled catenoids where the necks shrink to zero is not ULSC, whereas a sequence of rescaled helicoids is.

**Remark 12.1.** If each component of the intersection of a minimal surface with a ball of radius  $r_0$  is a disk, then so are the intersections with all sub-balls by the convex hull property (see, e.g., lemma C.1 in [19]). Therefore, it would be enough that (12.1) holds for  $r = r_0$ .

We will next describe briefly the case of ULSC sequences. See [20] for more on this and for the general case of fixed genus.

We will assume here that the surfaces are not disks (the case of disks was dealt with in the previous subsection). In particular, we will assume that for each  $i$ , there exists some  $y_i \in \mathbf{R}^3$  and  $s_i > 0$  so that

$$(12.2) \quad \text{some component of } B_{s_i}(y_i) \cap \Sigma_i \text{ is not a disk.}$$

Loosely speaking, the next result shows that when the sequence is ULSC (but not simply connected), a subsequence converges to a foliation by parallel planes away from two lines  $\mathcal{S}_1$  and  $\mathcal{S}_2$ ; see figure 10. The lines  $\mathcal{S}_1$  and  $\mathcal{S}_2$  are disjoint and orthogonal to the leaves of the foliation and the two lines are precisely the points where the curvature is blowing up. This is similar to the case of disks, except that we get two singular curves for non-disks as opposed to just one singular curve for disks.

**Theorem 12.2.** [20] *Let  $\Sigma_i \subset B_{R_i} = B_{R_i}(0) \subset \mathbf{R}^3$  be a sequence of compact embedded minimal surfaces with fixed genus and with  $\partial\Sigma_i \subset \partial B_{R_i}$  where  $R_i \rightarrow \infty$ . Suppose that each  $\Sigma_i$  is ULSC and satisfies (12.2) with  $s_i = R > 1$  and  $y_i = 0$ . If*

$$(12.3) \quad \sup_{B_1 \cap \Sigma_i} |A|^2 \rightarrow \infty,$$

*then there exists a subsequence  $\Sigma_j$ , two disjoint parallel lines  $\mathcal{S}_1$  and  $\mathcal{S}_2$ , and a rotation of  $\mathbf{R}^3$  so that:*

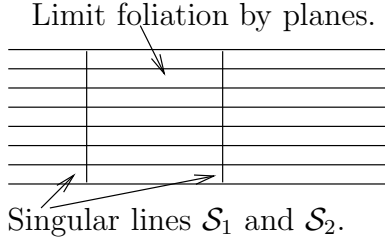
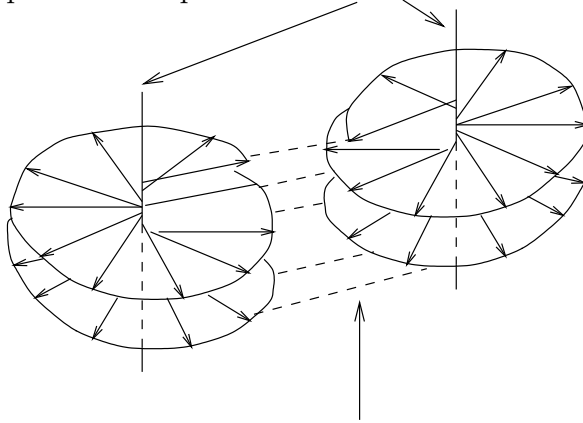


FIGURE 10. Theorem 12.2: Limits of sequences of non-simply connected, yet ULSC, surfaces with curvature blowing up. The singular set consists of two lines  $\mathcal{S}_1$  and  $\mathcal{S}_2$  and the limit is a foliation by flat parallel planes.

- (A) For each  $1 > \alpha > 0$ ,  $\Sigma_j \setminus (\mathcal{S}_1 \cup \mathcal{S}_2)$  converges in the  $C^\alpha$ -topology to the foliation  $\{x_3 = t\}$  by parallel planes.
- (B)  $\sup_{B_r(x) \cap \Sigma_j} |A|^2 \rightarrow \infty$  as  $j \rightarrow \infty$  for all  $r > 0$  and  $x \in \mathcal{S}_1 \cup \mathcal{S}_2$ . (The curvatures blow up along  $\mathcal{S}_1$  and  $\mathcal{S}_2$ .)
- ( $C_{ulsc}$ ) Away from  $\mathcal{S}_1 \cup \mathcal{S}_2$ , each  $\Sigma_j$  consists of exactly two multi-valued graphs spiraling together. Near  $\mathcal{S}_1$  and  $\mathcal{S}_2$ , the pair of multi-valued graphs form double spiral staircases with opposite orientations at  $\mathcal{S}_1$  and  $\mathcal{S}_2$ . Thus, circling only  $\mathcal{S}_1$  or only  $\mathcal{S}_2$  results in going either up or down, while a path circling both  $\mathcal{S}_1$  and  $\mathcal{S}_2$  closes up (see figure 11).
- ( $D_{ulsc}$ )  $\mathcal{S}_1$  and  $\mathcal{S}_2$  are orthogonal to the leaves of the foliation.

We should point out that the multi-valued graphs in ( $C_{ulsc}$ ) are defined over the doubly-punctured plane; see figure 11. The multi-valued graphs considered previously were defined over a plane punctured at just one point.

Locally graphical except over two points;  
those points correspond to the two axes.



The spiral staircases around each of the axes connect to each other between the axes.

FIGURE 11. A multi-valued graph over the doubly-punctured plane. The spiral staircases near each puncture are oppositely-oriented.

Despite the similarity of Theorem 12.2 to the case of disks, it is worth noting that the results for disks do not alone give this theorem. Namely, even though the ULSC sequence consists locally of disks, the compactness result for disks was in the global case where the radii go to infinity. One might wrongly think that Theorem 12.2 could be proven using the results for disks and a blow up argument. However, local examples constructed in [24] show the difficulty with such an argument.

**12.2. Fixed genus.** In the previous section, we analyzed sequences of embedded minimal surfaces with fixed genus where the topology does not concentrate at any points (i.e., ULSC sequences). We will now consider general sequences where the topology is allowed to concentrate. For simplicity, we will restrict to the case of genus zero, i.e., to planar domains (see [20] for the general case).

One way of locally distinguishing sequences where the topology does not concentrate from sequences where it does comes from analyzing the singular set. The singular set  $\mathcal{S}$  is defined to be the set of points where the curvature is blowing up. That is, a point  $y$  in  $\mathbf{R}^3$  is in  $\mathcal{S}$  for a sequence  $\Sigma_i$  if

$$(12.4) \quad \sup_{B_r(y) \cap \Sigma_i} |A|^2 \rightarrow \infty \text{ as } i \rightarrow \infty \text{ for all } r > 0.$$

For embedded minimal surfaces,  $\mathcal{S}$  consists of two types of points. The first type is roughly modelled on rescaled helicoids and the second on rescaled catenoids:

- A point  $y$  in  $\mathbf{R}^3$  is in  $\mathcal{S}_{ulsc}$  if the curvature for the sequence  $\Sigma_i$  blows up at  $y$  and the sequence is ULSC in a neighborhood of  $y$ .
- A point  $y$  in  $\mathbf{R}^3$  is in  $\mathcal{S}_{neck}$  if the sequence is not ULSC in any neighborhood of  $y$ . In this case, a sequence of closed non-contractible curves  $\gamma_i \subset \Sigma_i$  converges to  $y$ .

The sets  $\mathcal{S}_{neck}$  and  $\mathcal{S}_{ulsc}$  are obviously disjoint and the curvature blows up at both, so  $\mathcal{S}_{neck} \cup \mathcal{S}_{ulsc} \subset \mathcal{S}$ . An easy argument shows that, after passing to a subsequence, we can assume that

$$(12.5) \quad \mathcal{S} = \mathcal{S}_{neck} \cup \mathcal{S}_{ulsc}.$$

Note that  $\mathcal{S}_{neck} = \emptyset$  is equivalent to that the sequence is ULSC as is the case for sequences of rescaled helicoids. On the other hand,  $\mathcal{S}_{ulsc} = \emptyset$  for sequences of rescaled catenoids.

We will show that every sequence  $\Sigma_i$  has a subsequence that is either ULSC or for which  $\mathcal{S}_{ulsc}$  is empty. This is the next “no mixing” theorem. These two different cases give two very different structures.

**Theorem 12.3.** [20] *If  $\Sigma_i \subset B_{R_i} = B_{R_i}(0) \subset \mathbf{R}^3$  is a sequence of compact embedded minimal planar domains with  $\partial\Sigma_i \subset \partial B_{R_i}$  where  $R_i \rightarrow \infty$ , then there is a subsequence with either  $\mathcal{S}_{ulsc} = \emptyset$  or  $\mathcal{S}_{neck} = \emptyset$ .*

The case where  $\mathcal{S}_{neck} = \emptyset$  was dealt with in the previous section.

Common for both the ULSC case and the case where  $\mathcal{S}_{ulsc}$  is empty is that the limits are always laminations by flat parallel planes and the singular sets are always closed subsets contained in the union of the planes. This is the content of the next theorem:

**Theorem 12.4.** [20] *Let  $\Sigma_i \subset B_{R_i} = B_{R_i}(0) \subset \mathbf{R}^3$  be a sequence of compact embedded minimal surfaces with fixed genus and with  $\partial\Sigma_i \subset \partial B_{R_i}$  where  $R_i \rightarrow \infty$ .*

If

$$(12.6) \quad \sup_{B_1 \cap \Sigma_i} |A|^2 \rightarrow \infty,$$

then there exists a subsequence  $\Sigma_j$ , a lamination  $\mathcal{L} = \{x_3 = t\}_{t \in \mathcal{I}}$  of  $\mathbf{R}^3$  by parallel planes (where  $\mathcal{I} \subset \mathbf{R}$  is a closed set), and a closed nonempty set  $\mathcal{S}$  in the union of the leaves of  $\mathcal{L}$  such that after a rotation of  $\mathbf{R}^3$ :

- (A) For each  $1 > \alpha > 0$ ,  $\Sigma_j \setminus \mathcal{S}$  converges in the  $C^\alpha$ -topology to the lamination  $\mathcal{L} \setminus \mathcal{S}$ .
- (B)  $\sup_{B_r(x) \cap \Sigma_j} |A|^2 \rightarrow \infty$  as  $j \rightarrow \infty$  for all  $r > 0$  and  $x \in \mathcal{S}$ . (The curvatures blow up along  $\mathcal{S}$ .)

One can get both types of curvature blow-up by considering the family of embedded minimal planar domains known as the Riemann examples. Modulo translations and rotations, this is a two-parameter family of periodic minimal surfaces, where the parameters can be thought of as the size of the necks and the angle from one fundamental domain to the next. By choosing the two parameters appropriately, one can produce sequences of Riemann examples that illustrate both of the two structure theorems (cf. figures 8 and 9):

- (1) If we take a sequence of Riemann examples where the neck size is fixed and the angles go to  $\frac{\pi}{2}$ , then the surfaces with angle near  $\frac{\pi}{2}$  can be obtained by gluing together two oppositely-oriented double spiral staircases. Each double spiral staircase looks like a helicoid. This sequence of Riemann examples converges to a foliation by parallel planes. The convergence is smooth away from the axes of the two helicoids (these two axes are the singular set  $\mathcal{S}$  where the curvature blows up). The sequence is ULSC since the size of the necks is fixed and thus illustrates the first structure theorem, Theorem 12.2.
- (2) If we take a sequence of examples where the neck sizes go to zero, then we get a sequence that is *not* ULSC. However, the surfaces can be cut along short curves into collections of graphical pairs of pants. The short curves converge to points and the graphical pieces converge to flat planes except at these points, illustrating the second structure theorem, Theorem 12.5 below.

With these examples in mind, we are now ready to state our second main structure theorem describing the case where  $\mathcal{S}_{ulsc}$  is empty.

**Theorem 12.5.** *Let a sequence  $\Sigma_i$ , limit lamination  $\mathcal{L}$ , and singular set  $\mathcal{S}$  be as in Theorem 12.4. If  $\mathcal{S}_{ulsc} = \emptyset$  and*

$$(12.7) \quad \sup_{B_1 \cap \Sigma_i} |A|^2 \rightarrow \infty,$$

then  $\mathcal{S} = \mathcal{S}_{neck}$  by (12.5) and

- ( $C_{neck}$ ) *Each point  $y$  in  $\mathcal{S}$  comes with a sequence of graphs in  $\Sigma_j$  that converge to the plane  $\{x_3 = x_3(y)\}$ . The convergence is in the  $C^\infty$  topology away from the point  $y$  and possibly also one other point in  $\{x_3 = x_3(y)\} \cap \mathcal{S}$ . If the convergence is away from one point, then these graphs are defined over annuli; if the convergence is away from two points, then the graphs are defined over disks with two subdisks removed.*



### Part 3. Global theory of minimal surfaces in $\mathbf{R}^3$

**13.1. Minimal surfaces with finite total curvature.** A complete, non-compact, minimal immersion of a surface  $\Sigma$  in  $\mathbf{R}^3$  is said to have *finite total curvature* (or ftc) if

$$(13.1) \quad \int_{\Sigma} |A|^2 < \infty.$$

The simplest examples are the plane (where the total curvature is zero) and the catenoid. In the case of the catenoid, the Gauss map gives a conformal diffeomorphism to the sphere punctured at the north and south poles. Since  $A$  is the differential of the Gauss map, it follows that the catenoid has total curvature  $8\pi$ .

The fundamental result for minimal surfaces with ftc is that they are all conformally diffeomorphic to compact Riemann surfaces with a finite number of points removed. Namely, we have the following result of R. Osserman (see [79]):

**Theorem 13.1.** *Let  $\Sigma \subset \mathbf{R}^3$  be a complete minimal immersion with finite total curvature. Then:*

- (1)  $\Sigma$  is conformally diffeomorphic to a compact Riemann surface with a finite set of points removed. Each point corresponds to an end of the surface.
- (2)  $\Sigma$  is proper.
- (3) The Weierstrass data extends across the punctures meromorphically. (See Section 17 for the definition of the Weierstrass representation.)
- (4) The total curvature is an integral multiple of  $8\pi$ .

One application of this theorem is a classification of the ends of an embedded minimal surface with finite total curvature. Namely, one can show that any such end is asymptotic to either a plane or to half of a catenoid.

**13.2. The uniqueness of the catenoid.** Given the structure result, Theorem 13.1, it is natural to try to understand the space of minimal surfaces with finite total curvature in terms of the genus and the number of ends. Two such results were proven by R. Schoen and F. Lopez–A. Ros, respectively. The theorem of Schoen says that the catenoid is the unique embedded minimal surface with finite total curvature and exactly two ends.

**Theorem 13.2.** [89] *If  $\Sigma \subset \mathbf{R}^3$  is a connected embedded minimal surface with finite total curvature and exactly two ends, then  $\Sigma$  is a catenoid.*

The theorem of Lopez and Ros says that the catenoid and the plane are the only embedded minimal surfaces with finite total curvature and genus zero. Here, “genus zero” means conformal to the sphere with a finite set of points removed.

**Theorem 13.3.** [59] *If  $\Sigma \subset \mathbf{R}^3$  is an embedded minimal surface with finite total curvature and genus zero, then  $\Sigma$  is a catenoid or a plane.*

## 14. GLOBAL THEORY OF EMBEDDED MINIMAL SURFACES

Recent years have seen breakthroughs on many long-standing problems in the global theory of minimal surfaces in  $\mathbf{R}^3$ . This is an enormous subject and, rather than give a comprehensive treatment, we will mention a few important results which fit well with the rest of this survey. Throughout this section,  $\Sigma$  will be a complete

properly embedded minimal surface in  $\mathbf{R}^3$  (recall that properness here means that the intersection of  $\Sigma$  with any compact subset of  $\mathbf{R}^3$  is compact).

We say that  $\Sigma$  has finite topology if it is homeomorphic to a closed Riemann surface with a finite number of punctures; the genus of  $\Sigma$  is then the genus of this Riemann surface and the number of punctures is the number of ends. It follows that a neighborhood of each puncture corresponds to a properly embedded annular end of  $\Sigma$ . Perhaps surprisingly at first, the more restrictive case is when  $\Sigma$  has more than one end. The reason for this is that a barrier argument gives a stable minimal surface between any pair of ends. Such a stable surface is then asymptotic to a plane (or catenoid), essentially forcing each end to live in a half-space. Using this restriction, P. Collin proved:

**Theorem 14.1.** [30] *Each end of a complete properly embedded minimal surface with finite topology and at least two ends is asymptotic to a plane or catenoid.*

In particular, outside some compact set,  $\Sigma$  is given by a finite collection of disjoint graphs over a common plane (and has finite total curvature).

As mentioned above, Collin essentially proved Theorem 14.1 by showing that an embedded annular end that lives in a half-space must have finite total curvature. [27] used the one-sided curvature estimate to strengthen this from a half-space to a strictly larger cone, and in the process give a very different proof of Collin's theorem.

**Theorem 14.2.** [27] *There exists  $\epsilon > 0$  so that any complete properly embedded minimal annular end contained in the cone*

$$(14.1) \quad \{x_3 \geq -\epsilon(x_1^2 + x_2^2 + x_3^2)^{1/2}\}$$

*is asymptotic to a plane or catenoid.*

When  $\Sigma$  has only one end (e.g., for the helicoid), it need not have finite total curvature so the situation is more delicate. However, the regularity results of the previous section can be applied. For example, if  $\Sigma$  is a (non-planar) embedded minimal disk, then we get a multi-valued graph structure away from a “one-dimensional singular set.” Using Theorems 11.1 and 11.2, W. Meeks and H. Rosenberg proved the uniqueness of the helicoid:

**Theorem 14.3.** [70] *The plane and helicoid are the only complete properly embedded simply-connected minimal surfaces in  $\mathbf{R}^3$ .*

This uniqueness has many applications. Recall that if we take a sequence of rescalings of the helicoid, then the singular set  $\mathcal{S}$  for the convergence is the vertical axis perpendicular to the leaves of the foliation. In [64], W. Meeks used this fact together with the uniqueness of the helicoid to prove that the singular set  $\mathcal{S}$  in Theorem 11.1 is always a straight line perpendicular to the foliation. Recently, W. Meeks and M. Weber have constructed a *local* example (i.e., a sequence of embedded minimal disks in a unit ball) where  $\mathcal{S}$  is a circle.

We have not even touched on the case where  $\Sigma$  has infinite topology (e.g., when  $\Sigma$  is one of the Riemann examples). This is an area of much current research, see [18], the work of Meeks, J. Perez and A. Ros, [67], [68], and [69], the survey [66] and references therein.

We close this section with a local analog of the two-ended case. Namely, in [22], we proved that any embedded minimal annulus in a ball (with boundary in the boundary of the ball and) with a small neck can be decomposed by a simple closed geodesic into two graphical sub-annuli. Moreover, we gave a sharp bound for the length of this closed geodesic in terms of the separation (or height) between the graphical sub-annuli. This serves to illustrate our “pair of pants” decomposition from [18] in the special case where the embedded minimal planar domain is an annulus (we will not touch on this further here). The catenoid

$$(14.2) \quad \{x_1^2 + x_2^2 = \cosh^2 x_3\}$$

is the prime example of an embedded minimal annulus.

The precise statement of this decomposition for annuli is:

**Theorem 14.4.** [22] *There exist  $\epsilon > 0$ ,  $C_1, C_2, C_3 > 1$  so: If  $\Sigma \subset B_R \subset \mathbf{R}^3$  is an embedded minimal annulus with  $\partial\Sigma \subset \partial B_R$  and  $\pi_1(B_{\epsilon R} \cap \Sigma) \neq 0$ , then there exists a simple closed geodesic  $\gamma \subset \Sigma$  of length  $\ell$  so that:*

- *The curve  $\gamma$  splits the connected component of  $B_{R/C_1} \cap \Sigma$  containing it into two annuli  $\Sigma^+, \Sigma^-$  each with  $\int |A|^2 \leq 5\pi$ .*
- *Furthermore,  $\Sigma^\pm \setminus \mathcal{T}_{C_2 \ell}(\gamma)$  are graphs with gradient  $\leq 1$ .*
- *Finally,  $\ell \log(R/\ell) \leq C_3 h$  where the separation  $h$  is given by*

$$(14.3) \quad h = \min_{x_\pm \in \partial B_{R/C_1} \cap \Sigma^\pm} |x_+ - x_-|.$$

Here  $\mathcal{T}_s(S) \subset \Sigma$  denotes the intrinsic  $s$ -tubular neighborhood of a subset  $S \subset \Sigma$ .

## 15. THE CALABI-YAU CONJECTURES

Recall that an immersed submanifold in  $\mathbf{R}^n$  is *proper* if the pre-image of any compact subset of  $\mathbf{R}^n$  is compact in the surface. This property has played an important role in the theory of minimal submanifolds and many of the classical theorems in the subject assume that the submanifold is proper.

It is easy to see that any compact submanifold is automatically proper. On the other hand, there is no reason to expect a general immersion (or even embedding) to be proper. For example, the non-compact curve parametrized in polar coordinates by

$$(15.1) \quad \rho(t) = \pi + \arctan(t), \theta(t) = t$$

spirals infinitely between the circles of radius  $\pi/2$  and  $3\pi/2$ . However, it was long thought that a minimal immersion (or embedding) should be better behaved. This principle was captured by the Calabi-Yau conjectures, dating back to the 1960s. Much work has been done on them over the past four decades. Their original form was given in 1965 in [10] where E. Calabi made the following two conjectures about minimal surfaces (see also S.S. Chern, page 212 of [11] and S.T. Yau’s 1982 problem list):

**Conjecture 1.** *“Prove that a complete minimal hypersurface in  $\mathbf{R}^n$  must be unbounded.”*

Calabi continued: “It is known that there are no compact minimal submanifolds of  $\mathbf{R}^n$  (or of any simply connected complete Riemannian manifold with sectional curvature  $\leq 0$ ). A more ambitious conjecture is”:

**Conjecture 2.** “A complete [nonflat] minimal hypersurface in  $\mathbf{R}^n$  has an unbounded projection in every  $(n - 2)$ -dimensional flat subspace.”

The immersed versions of these conjectures turned out to be false. As mentioned above, Jorge and Xavier, [50], constructed nonflat minimal immersions contained between two parallel planes in 1980, giving a counter-example to the immersed version of the more ambitious Conjecture 2. Another significant development came in 1996, when N. Nadirashvili, [77], constructed a complete immersion of a minimal disk into the unit ball in  $\mathbf{R}^3$ , showing that Conjecture 1 also failed for immersed surfaces; see [60], [57], [58], for other topological types than disks.

It is clear from the definition of proper that a proper minimal surface in  $\mathbf{R}^3$  must be unbounded, so the examples of Nadirashvili are not proper. Much less obvious is that the plane is the only complete proper immersed minimal surface in a halfspace. This is however a consequence of the strong halfspace theorem of D. Hoffman and W. Meeks:

**Theorem 15.1.** [44] *A complete connected properly immersed minimal surface  $\Sigma \subset \{x_3 > 0\} \subset \mathbf{R}^3$  must be a horizontal plane  $\{x_3 = \text{Constant}\}$ .*

The main result of [29] is an effective version of properness for disks, giving a chord arc bound. Obviously, intrinsic distances are larger than extrinsic distances, so the significance of a chord arc bound is the reverse inequality, i.e., a bound on intrinsic distances from above by extrinsic distances. This is accomplished in the next theorem:

**Theorem 15.2.** [29] *There exists a constant  $C > 0$  so that if  $\Sigma \subset \mathbf{R}^3$  is an embedded minimal disk,  $\mathcal{B}_{2R} = \mathcal{B}_{2R}(0)$  is an intrinsic ball in  $\Sigma \setminus \partial\Sigma$  of radius  $2R$ , and  $\sup_{\mathcal{B}_{r_0}} |A|^2 > r_0^{-2}$  where  $R > r_0$ , then for  $x \in \mathcal{B}_R$*

$$(15.2) \quad C \operatorname{dist}_\Sigma(x, 0) < |x| + r_0.$$

The assumption of a lower curvature bound,  $\sup_{\mathcal{B}_{r_0}} |A|^2 > r_0^{-2}$ , in the theorem is a necessary normalization for a chord arc bound. This can easily be seen by rescaling and translating the helicoid.

Properness of a complete embedded minimal disk is an immediate consequence of Theorem 15.2. Namely, by (15.2), as intrinsic distances go to infinity, so do extrinsic distances. Precisely, if  $\Sigma$  is flat, and hence a plane, then obviously  $\Sigma$  is proper and if it is non-flat, then  $\sup_{\mathcal{B}_{r_0}} |A|^2 > r_0^{-2}$  for some  $r_0 > 0$  and hence  $\Sigma$  is proper by (15.2).

A consequence of Theorem 15.2 together with the one-sided curvature estimate of [19] (i.e., theorem 0.2 in [19]) is the following version of that estimate for intrinsic balls:

**Corollary 15.3.** [29] *There exists  $\epsilon > 0$ , so that if*

$$(15.3) \quad \Sigma \subset \{x_3 > 0\} \subset \mathbf{R}^3$$

*is an embedded minimal disk with  $\mathcal{B}_{2R}(x) \subset \Sigma \setminus \partial\Sigma$  and  $|x| < \epsilon R$ , then*

$$(15.4) \quad \sup_{\mathcal{B}_R(x)} |A_\Sigma|^2 \leq R^{-2}.$$

As a corollary of this intrinsic one-sided curvature estimate we get that the second, and more ambitious, of Calabi’s conjectures is also true for embedded minimal disks.

In fact, [29] proved both of Calabi’s conjectures and properness also for embedded surfaces with finite topology. Recall that a surface  $\Sigma$  is said to have finite topology if it is homeomorphic to a closed Riemann surface with a finite set of points removed or “punctures”. Each puncture corresponds to an end of  $\Sigma$ .

The following generalization of the halfspace theorem gives Calabi’s second, more ambitious, conjecture for embedded surfaces with finite topology:

**Theorem 15.4.** *The plane is the only complete embedded minimal surface with finite topology in  $\mathbf{R}^3$  in a halfspace.*

Likewise, we get the properness of embedded surfaces with finite topology:

**Theorem 15.5.** *A complete embedded minimal surface with finite topology in  $\mathbf{R}^3$  must be proper.*

Compare also W. Meeks and H. Rosenberg, [71].

There has been extensive work on both properness and the halfspace property assuming various curvature bounds. Jorge and Xavier, [49] and [50], showed that there cannot exist a complete immersed minimal surface with bounded curvature in  $\cap_i \{x_i > 0\}$ ; later Xavier proved that the plane is the only such surface in a halfspace, [107]. Recently, G.P. Bessa, Jorge and G. Oliveira-Filho, [7], and H. Rosenberg, [86], have shown that if such a surface is embedded, then it must be proper. This properness was extended to embedded minimal surfaces with locally bounded curvature and finite topology by Meeks and Rosenberg in [70]; finite topology was subsequently replaced by finite genus in [67] by Meeks, J. Perez and A. Ros.

Inspired by Nadirashvili’s examples, F. Martin and S. Morales constructed in [61] a complete bounded minimal immersion which is proper in the (open) unit ball. That is, the preimages of compact subsets of the (open) unit ball are compact in the surface and the image of the surface accumulates on the boundary of the unit ball. They extended this in [62] to show that any convex, possibly noncompact or nonsmooth, region of  $\mathbf{R}^3$  admits a proper complete minimal immersion of the unit disk; cf. [78].

#### Part 4. Constructing minimal surfaces

Thus far, we have mainly dealt with regularity and *a priori* estimates but have ignored questions of existence. In this part we survey some of the most useful existence results for minimal surfaces. Section 16 gives an overview of the classical Plateau problem. Section 17 recalls the classical Weierstrass representation, including a few modern applications, and the Kapouleas desingularization method. Section 18 deals with producing area minimizing surfaces and questions of embeddedness. Finally, Section 19 recalls the min–max construction for producing unstable minimal surfaces and, in particular, doing so while controlling the topology and guaranteeing embeddedness.

### 16. THE PLATEAU PROBLEM

The following fundamental existence problem for minimal surfaces is known as the *Plateau problem*: Given a closed curve  $\Gamma$ , find a minimal surface with boundary  $\Gamma$ . There are various solutions to this problem depending on the exact definition of a

surface (parameterized disk, integral current,  $\mathbf{Z}_2$  current, or rectifiable varifold). We shall consider the version of the Plateau problem for parameterized disks; this was solved independently by J. Douglas and T. Rado. The generalization to Riemannian manifolds is due to C. B. Morrey.

**Theorem 16.1.** *Let  $\Gamma \subset \mathbf{R}^3$  be a piecewise  $C^1$  closed Jordan curve. Then there exists a piecewise  $C^1$  map  $u$  from  $D \subset \mathbf{R}^2$  to  $\mathbf{R}^3$  with  $u(\partial D) \subset \Gamma$  such that the image minimizes area among all disks with boundary  $\Gamma$ .*

The solution  $u$  to the Plateau problem above can easily be seen to be a branched conformal immersion. R. Osserman proved that  $u$  does not have true interior branch points; subsequently, R. Gulliver and W. Alt showed that  $u$  cannot have false branch points either.

Furthermore, the solution  $u$  is as smooth as the boundary curve, even up to the boundary. A very general version of this boundary regularity was proven by S. Hildebrandt; for the case of surfaces in  $\mathbf{R}^3$ , recall the following result of J. C. C. Nitsche:

**Theorem 16.2.** *If  $\Gamma$  is a regular Jordan curve of class  $C^{k,\alpha}$  where  $k \geq 1$  and  $0 < \alpha < 1$ , then a solution  $u$  of the Plateau problem is  $C^{k,\alpha}$  on all of  $\bar{D}$ .*

The optimal boundary regularity theorem in higher dimensions was proven by R. Hardt and L. Simon in [40].

## 17. THE WEIERSTRASS REPRESENTATION

The classical *Weierstrass representation* (see [43] or [79]) takes holomorphic data (a Riemann surface, a meromorphic function, and a holomorphic one-form) and associates to these data a minimal surface in  $\mathbf{R}^3$ . To be precise, given a Riemann surface  $\Omega$ , a meromorphic function  $g$  on  $\Omega$ , and a holomorphic one-form  $\phi$  on  $\Omega$ , then we get a (branched) conformal minimal immersion  $F : \Omega \rightarrow \mathbf{R}^3$  by

$$(17.1) \quad F(z) = \operatorname{Re} \int_{\zeta \in \gamma_{z_0,z}} \left( \frac{1}{2} (g^{-1}(\zeta) - g(\zeta)), \frac{i}{2} (g^{-1}(\zeta) + g(\zeta)), 1 \right) \phi(\zeta).$$

Here  $z_0 \in \Omega$  is a fixed base point and the integration is along a path  $\gamma_{z_0,z}$  from  $z_0$  to  $z$ . The choice of  $z_0$  changes  $F$  by adding a constant. In general, the map  $F$  may depend on the choice of path (and hence may not be well-defined); this is known as “the period problem” (see M. Weber and M. Wolf, [104], for the latest developments). However, when  $g$  has no zeros or poles and  $\Omega$  is simply connected, then  $F(z)$  does not depend on the choice of path  $\gamma_{z_0,z}$ .

Three standard constructions of minimal surfaces from Weierstrass data are

$$(17.2) \quad g(z) = z, \phi(z) = dz/z, \Omega = \mathbf{C} \setminus \{0\} \text{ giving a catenoid,}$$

$$(17.3) \quad g(z) = z, \phi(z) = z dz, \Omega = \mathbf{C} \text{ giving Enneper's surface,}$$

$$(17.4) \quad g(z) = e^{iz}, \phi(z) = dz, \Omega = \mathbf{C} \text{ giving a helicoid.}$$

The Weierstrass representation is particularly useful for constructing immersed minimal surfaces. For example, in [77], N. Nadirashvili used it to construct a complete immersed minimal surface in the unit ball in  $\mathbf{R}^3$  (see also [50] for the case of a slab). In particular, Nadirashvili’s surface is not proper, i.e., the intersections with compact sets are not necessarily compact.

Typically, it is rather difficult to prove that the resulting immersion is an embedding (i.e., is 1–1), although there are some interesting cases where this can be done. The first modern example was [44] where D. Hoffman and W. Meeks proved that the surface constructed by Costa was embedded; this was the first new complete finite topology properly embedded minimal surface discovered since the classical catenoid, helicoid, and plane. This led to the discovery of many more such surfaces (see [43] and [84] for more discussion).

Very recently in [45] (see also [46]), D. Hoffman, M. Weber, and M. Wolf have used the Weierstrass representation to construct a genus one properly embedded minimal surface asymptotic to the helicoid. They construct this “genus one helicoid” as the limit of a continuous one-parameter family of screw-motion invariant minimal surfaces—also asymptotic to the helicoid—that have genus equal to one in the quotient.

In [24], we used the Weierstrass representation to construct a sequence of embedded minimal disks

$$(17.5) \quad \Sigma_i \subset B_1 = B_1(0) \subset \mathbf{R}^3$$

with  $\partial\Sigma_i \subset \partial B_1$  where the curvatures blow up only at 0 and  $\Sigma_i \setminus \{x_3\text{-axis}\}$  consists of two multi-valued graphs for each  $i$ . Furthermore,  $\Sigma_i \setminus \{x_3 = 0\}$  converges to two embedded minimal disks  $\Sigma^- \subset \{x_3 < 0\}$  and  $\Sigma^+ \subset \{x_3 > 0\}$  each of which spirals into  $\{x_3 = 0\}$  and thus is not proper. (This should be contrasted with Theorem 11.1 where the *complete* limits are planes and hence proper.)

N. Kapouleas has developed another method to construct complete embedded minimal surfaces with finite total curvature. For instance, in [54], he shows that (most) collections of coaxial catenoids and planes can be desingularized to get complete embedded minimal surfaces with finite total curvature. The Costa surface above had genus one and three ends (that is to say, it is homeomorphic to a torus with three punctures). In the Kapouleas construction, one could start with a plane and catenoid intersecting in a circle and then desingularize this circle using suitably scaled and bent Scherk surfaces to get a finite genus embedded surface with three ends. (This desingularization process adds handles, i.e., increases the genus.) In this manner, Kapouleas gets an enormous number of new examples; see also the gluing construction of S.D. Yang, [108], which uses catenoid necks to glue together nearby minimal surfaces.

## 18. AREA-MINIMIZING SURFACES

Perhaps the most natural way to construct minimal surfaces is to look for ones which minimize area, e.g., with fixed boundary, or in a homotopy class, etc. This has the advantage that often it is possible to show that the resulting surface is embedded. We mention a few results along these lines.

The first embeddedness result, due to W. Meeks and S.T. Yau, shows that if the boundary curve is embedded and lies on the boundary of a smooth mean convex set (and it is null-homotopic in this set), then it bounds an embedded least area disk.

**Theorem 18.1.** [74] *Let  $M^3$  be a compact Riemannian three-manifold whose boundary is mean convex and let  $\gamma$  be a simple closed curve in  $\partial M$  which is null-homotopic in  $M$ ; then  $\gamma$  is bounded by a least area disk and any such least area disk is properly embedded.*



Note that some restriction on the boundary curve  $\gamma$  is certainly necessary. For instance, if the boundary curve was knotted (e.g., the trefoil), then it could not be spanned by any embedded disk (minimal or otherwise). Prior to the work of Meeks and Yau, embeddedness was known for extremal boundary curves in  $\mathbf{R}^3$  with small total curvature by the work of R. Gulliver and J. Spruck [38]; see chapter 4 in [14] for other results and further discussion. Recently, in [33], T. Ekholm, B. White, and D. Wienholtz proved that minimal surfaces whose boundary has total curvature less than  $4\pi$  also must be embedded.

If we instead fix a homotopy class of maps, then the two fundamental existence results are due to J. Sacks–K. Uhlenbeck and R. Schoen–S.T. Yau (with embeddedness proven by W. Meeks–S.T. Yau and M. Freedman–J. Hass–P. Scott, respectively):

**Theorem 18.2.** [87], [75] *Given  $M^3$ , there exist conformal (stable) minimal immersions  $u_1, \dots, u_m : \mathbf{S}^2 \rightarrow M$  which generate  $\pi_2(M)$  as a  $\mathbf{Z}[\pi_1(M)]$  module. Furthermore,*

- *If  $u : \mathbf{S}^2 \rightarrow M$  and  $[u]_{\pi_2} \neq 0$ , then  $\text{Area}(u) \geq \min_i \text{Area}(u_i)$ .*
- *Each  $u_i$  is either an embedding or a 2–1 map onto an embedded 2–sided  $\mathbf{R}P^2$ .*

**Theorem 18.3.** [93], [36] *If  $\Sigma^2$  is a closed surface with genus  $g > 0$  and  $i_0 : \Sigma \rightarrow M^3$  is an embedding which induces an injective map on  $\pi_1$ , then there is a least area embedding with the same action on  $\pi_1$ .*

In [72], W. Meeks, L. Simon, and S.T. Yau find an embedded sphere minimizing area in an isotopy class in a closed 3–manifold.

We end this section by mentioning two applications of Theorem 18.3. First, in [26], we showed that any topological 3–manifold  $M$  had an open set of metrics so that, for each such metric, there was a sequence of embedded minimal tori whose area went to infinity. In [32], B. Dean showed that this was true for every genus  $g \geq 1$ .

## 19. THE MIN–MAX CONSTRUCTION OF MINIMAL SURFACES

Variational arguments can also be used to construct higher index (i.e., non–minimizing) minimal surfaces using the topology of the space of surfaces. There are two basic approaches:

- Applying Morse theory to the energy functional on the space of maps from a fixed surface  $\Sigma$  to  $M$ .
- Doing a min–max argument over families of (topologically non–trivial) sweep–outs of  $M$ .

The first approach has the advantage that the topological type of the minimal surface is easily fixed; however, the second approach has been more successful at producing embedded minimal surfaces. We will highlight a few key results below but refer to [13] for a thorough treatment.

Unfortunately, one cannot directly apply Morse theory to the energy functional on the space of maps from a fixed surface because of a lack of compactness (the Palais–Smale Condition C does not hold). To get around this difficulty, J. Sacks and K. Uhlenbeck, [87], introduce a family of perturbed energy functionals which



do satisfy Condition C and then obtain minimal surfaces as limits of critical points for the perturbed problems:

**Theorem 19.1.** [87] *If  $\pi_k(M) \neq 0$  for some  $k > 1$ , then there exists a branched immersed minimal 2-sphere in  $M$  (for any metric).*

This was sharpened somewhat by M. Micalef and D. Moore, [76], (showing that the index of the minimal sphere was at most  $k - 2$ ), who used it to prove a generalization of the sphere theorem. See A. Fraser, [37], for a generalization to a free boundary problem.

The basic idea of constructing minimal surfaces via min-max arguments and sweep-outs goes back to G. Birkhoff, who developed it to construct simple closed geodesics on spheres. In particular, when  $M$  is a topological 2-sphere, we can find a 1-parameter family of curves starting and ending at point curves so that the induced map  $F : \mathbf{S}^2 \rightarrow \mathbf{S}^2$  (see figure 12) has nonzero degree. The min-max argument produces a nontrivial closed geodesic of length less than or equal to the longest curve in the initial one-parameter family. A curve shortening argument gives that the geodesic obtained in this way is simple.

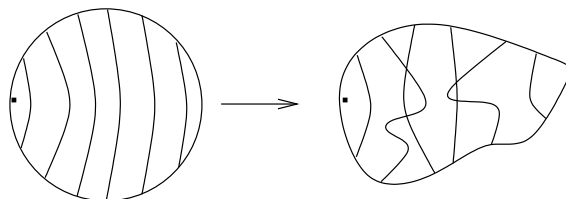


FIGURE 12. A 1-parameter family of curves on a 2-sphere which induces a map  $F : \mathbf{S}^2 \rightarrow \mathbf{S}^2$  of degree 1. First published in *Surveys in Differential Geometry*, volume IX, in 2004, published by International Press.

In [82], J. Pitts applied a similar argument and geometric measure theory to get that every closed Riemannian three manifold has an embedded minimal surface (his argument was for dimensions up to seven), but he did not estimate the genus of the resulting surface. Finally, F. Smith (under the direction of L. Simon) proved (see [13]):

**Theorem 19.2.** [99] *Every metric on a topological 3-sphere  $M$  admits an embedded minimal 2-sphere.*

The main new contribution of Smith was to control the topological type of the resulting minimal surface while keeping it embedded; see also J. Pitts and J.H. Rubinstein, [83], for some generalizations.

## Part 5. Some applications of minimal surfaces

In this last part, we discuss very briefly a few applications of minimal surfaces. As mentioned in the introduction, there are many to choose from and we have selected just a few. See [4], [35], [39], [42], [101], and [102] for other applications.

**20.1. The positive mass theorem.** The (Riemannian version of the) *positive mass theorem* of R. Schoen and S.T. Yau states that an asymptotically flat 3-manifold  $M$  with non-negative scalar curvature must have positive mass. The Riemannian manifold  $M$  here arises as a maximal space-like slice in a 3+1-dimensional space-time solution of Einstein's equations.

The asymptotic flatness of  $M$  comes from that the space-time models an isolated gravitational system and hence is a perturbation of the vacuum solution outside a large compact set. To make this precise, suppose for simplicity that  $M$  has only one end;  $M$  is then said to be *asymptotically flat* if there is a compact set  $\Omega \subset M$  so that  $M \setminus \Omega$  is diffeomorphic to  $\mathbf{R}^3 \setminus B_R(0)$  and the metric on  $M \setminus \Omega$  can be written as

$$(20.1) \quad g_{ij} = \left(1 + \frac{\mathcal{M}}{2|x|}\right)^4 \delta_{ij} + p_{ij},$$

where

$$(20.2) \quad |x|^2 |p_{ij}| + |x|^3 |D p_{ij}| + |x|^4 |D^2 p_{ij}| \leq C.$$

The constant  $\mathcal{M}$  is the so called *mass* of  $M$ . Observe that the metric  $g_{ij}$  is a perturbation of the metric on a constant-time slice in the Schwarzschild space-time of mass  $\mathcal{M}$ ; that is to say, the Schwarzschild metric has  $p_{ij} \equiv 0$ .

A tensor  $h$  is said to be  $O(|x|^{-p})$  if  $|x|^p |h| + |x|^{p+1} |D h| \leq C$ . For example, an easy calculation shows that

$$(20.3) \quad \begin{aligned} g_{ij} &= (1 + 2\mathcal{M}/|x|) \delta_{ij} + O(|x|^{-2}), \\ \sqrt{g} &\equiv \sqrt{\det g_{ij}} = 1 + 3\mathcal{M}|x|^{-1} + O(|x|^{-2}). \end{aligned}$$

The positive mass theorem states that the mass  $\mathcal{M}$  of such an  $M$  must be non-negative:

**Theorem 20.1.** [92] *With  $M$  as above,  $\mathcal{M} \geq 0$ .*

There is a rigidity theorem as well which states that the mass vanishes only when  $M$  is isometric to  $\mathbf{R}^3$ :

**Theorem 20.2.** [92] *If  $|\nabla^3 p_{ij}| = O(|x|^{-5})$  and  $\mathcal{M} = 0$  in Theorem 20.1, then  $M$  is isometric to  $\mathbf{R}^3$ .*

We will give a very brief overview of the proof of Theorem 20.1, showing in the process where minimal surfaces appear.

*Proof.* (Sketch.) The argument will be by contradiction, so suppose that the mass is negative. Note first that a ‘‘rounding off’’ argument shows that the metric on  $M$  can be perturbed to have positive scalar curvature outside of a compact set and still have negative mass.

It is not hard to prove that the slab between two parallel planes is mean-convex. That is, we have the following:

**Lemma 20.3.** *If  $\mathcal{M} < 0$  and  $M$  is asymptotically flat, then there exist  $R_0, h > 0$  so that for  $r > R_0$  the sets*

$$(20.4) \quad C_r = \{|x|^2 \leq r^2, -h \leq x_3 \leq h\}$$

*have strictly mean convex boundary.*

Since the compact set  $C_r$  is mean convex, we can solve the Plateau problem (as in Section 16) to get an area minimizing (and hence stable) surface  $\Gamma_r \subset C_r$  with boundary

$$(20.5) \quad \partial\Gamma_r = \{|x|^2 = r^2, x_3 = h\}.$$

Using the disk  $\{|x|^2 \leq r^2, x_3 = h\}$  as a comparison surface, we get uniform local area bounds for any such  $\Gamma_r$ . Combining these local area bounds with the *a priori* curvature estimates for minimizing surfaces, we can take a sequence of  $r$ 's going to infinity and find a subsequence of  $\Gamma_r$ 's that converge to a complete area-minimizing surface

$$(20.6) \quad \Gamma \subset \{-h \leq x_3 \leq h\}.$$

Since  $\Gamma$  is pinched between the planes  $\{x_3 = \pm h\}$ , the estimates for minimizing surfaces implies that (outside a large compact set)  $\Gamma$  is a graph over the plane  $\{x_3 = 0\}$  and hence has quadratic area growth and finite total curvature. Moreover, using the form of the metric  $g_{ij}$ , we see that  $|\nabla u|$  decays like  $|x|^{-1}$  and

$$(20.7) \quad \int_{\sigma_s} k_g = (2\pi s + O(1))(s^{-1} + O(s^{-2})) = 2\pi + O(s^{-1}),$$

where  $\sigma_s$  is the curve  $\{x_1^2 + x_2^2 = s^2\} \cap \Gamma$  and  $k_g$  is the geodesic curvature of  $\sigma_s$  (considered as a curve in the surface  $\Gamma$ ).

To get the contradiction, one combines stability of  $\Gamma$  with the positive scalar curvature of  $M$  to see that no such  $\Gamma$  could have existed. Namely, substituting the Gauss equation into the stability inequality in a general 3-manifold (see, e.g., [14]) gives

$$(20.8) \quad \int_{\Gamma} (|A|^2/2 + \text{Scal}_M - K_{\Sigma})\phi^2 \leq \int_{\Gamma} |\nabla\phi|^2.$$

Since  $\Gamma$  has quadratic area growth, we can choose a sequence of (logarithmic) cutoff functions in (20.8) to get

$$(20.9) \quad 0 < \int_{\Sigma} (|A|^2/2 + \text{Scal}_M) \leq \int_{\Sigma} K_{\Sigma} < \infty;$$

since  $K_{\Sigma}$  may not be positive, we also used that  $\Gamma$  has finite total curvature. Moreover, we used that  $\text{Scal}_M$  is positive outside a compact set to see that the first integral in (20.9) was positive. Finally, substituting (20.9) into the Gauss-Bonnet formula gives that  $\int_{\sigma_s} k_g$  is strictly less than  $2\pi$  for  $s$  large, contradicting (20.7).  $\square$

**20.2. Black holes.** Another way that minimal surfaces enter into relativity is through black holes. Suppose that we have a three-dimensional time-slice  $M$  in a  $3 + 1$ -dimensional space-time. For simplicity, assume that  $M$  is totally geodesic and hence has non-negative scalar curvature. A closed surface  $\Sigma$  in  $M$  is said to be trapped if its mean curvature is everywhere negative with respect to its outward normal. Physically, this means that the surface emits an outward shell of light whose surface area is decreasing everywhere on the surface. The existence of a closed trapped surface implies the existence of a black hole in the space-time.

Given a trapped surface, we can look for the outermost trapped surface containing it; this outermost surface is called an apparent horizon. It is not hard to see that an apparent horizon must be a minimal surface and, moreover, a barrier argument shows that it must be stable. Since  $M$  has non-negative scalar curvature,

stability in turn implies that it must be diffeomorphic to a sphere. See, for instance, [9] and [47] for some results on black holes, horizons, etc.

**20.3. Constant mean curvature surfaces.** At least since the time of Plateau, minimal surfaces have been used to model soap films. This is because the mean curvature of the surface models the surface tension and this is essentially the only force acting on a soap film. Soap bubbles, on other hand, enclose a volume and thus the pressure gives a second counterbalancing force. It follows easily that these two forces are in equilibrium when the surface has constant mean curvature.

For the same reason, constant mean curvature surfaces arise in the isoperimetric problem. Namely, a surface that minimizes surface area while enclosing a fixed volume must have constant mean curvature (or “cmc”). It is not hard to see that such an isoperimetric surface in  $\mathbf{R}^n$  must be a round sphere. There are two interesting partial converses to this. First, by a theorem of H. Hopf, any cmc 2-sphere in  $\mathbf{R}^3$  must be round. Second, using the maximum principle (“the method of moving planes”) A.D. Alexandrov showed that any closed embedded cmc hypersurface in  $\mathbf{R}^n$  must be a round sphere. It turned out, however, that not every closed immersed cmc surface is round. The first examples were immersed cmc tori constructed by H. Wente, [105]. N. Kapouleas constructed many new examples, including closed higher genus cmc surfaces, [52], [53]. See also [63] and [55] for other results on the space of such cmc surfaces.

Many of the techniques developed for studying minimal surfaces generalize to general constant mean curvature surfaces.

**20.4. Finite extinction for Ricci flow.** We close this survey with indicating how minimal surfaces can be used to show that on a homotopy 3-sphere the Ricci flow become extinct in finite time (see [25], [80] for details).

Let  $M^3$  be a smooth closed orientable 3-manifold and let  $g(t)$  be a one-parameter family of metrics on  $M$  evolving by the Ricci flow, so

$$(20.10) \quad \partial_t g = -2 \operatorname{Ric}_{M_t} .$$

In an earlier section, we saw that there is a natural way of constructing minimal surfaces on many 3-manifolds and that comes from the min-max argument where the minimal of all maximal slices of sweep-outs is a minimal surface. The idea is then to look at how the area of this min-max surface changes under the flow. Geometrically the area measures a kind of width of the 3-manifold and as we will see for certain 3-manifolds (those, like the 3-sphere, whose prime decomposition contains no aspherical factors) the area becomes zero in finite time corresponding to that the solution becomes extinct in finite time.

Fix a continuous map  $\beta : [0, 1] \rightarrow C^0 \cap L^2_1(\mathbf{S}^2, M)$  where  $\beta(0)$  and  $\beta(1)$  are constant maps so that  $\beta$  is in the nontrivial homotopy class  $[\beta]$  (such  $\beta$  exists when  $M$  is a homotopy 3-sphere). We define the width  $W = W(g, [\beta])$  by

$$(20.11) \quad W(g) = \min_{\gamma \in [\beta]} \max_{s \in [0, 1]} \operatorname{Energy}(\gamma(s)) .$$

The next theorem gives an upper bound for the derivative of  $W(g(t))$  under the Ricci flow which forces the solution  $g(t)$  to become extinct in finite.

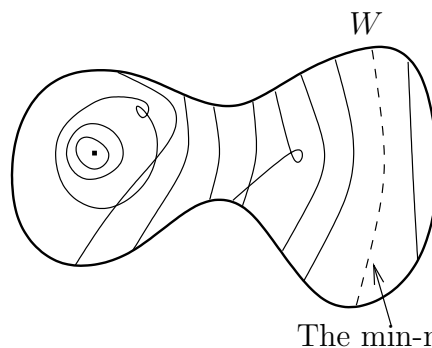


FIGURE 13. The sweep-out, the min-max surface, and the width  $W$ . First published in the Journal of the American Mathematical Society in 2005, published by the American Mathematical Society.

**Theorem 20.4.** *Let  $M^3$  be a homotopy 3-sphere equipped with a Riemannian metric  $g = g(0)$ . Under the Ricci flow, the width  $W(g(t))$  satisfies*

$$(20.12) \quad \frac{d}{dt} W(g(t)) \leq -4\pi + \frac{3}{4(t+C)} W(g(t)),$$

*in the sense of the limsup of forward difference quotients. Hence,  $g(t)$  must become extinct in finite time.*

The  $4\pi$  in (20.12) comes from the Gauss–Bonnet theorem and the  $3/4$  comes from the bound on the minimum of the scalar curvature that the evolution equation implies. Both of these constants matter whereas the constant  $C$  depends on the initial metric and the actual value is not important.

To see that (20.12) implies finite extinction time rewrite (20.12) as

$$(20.13) \quad \frac{d}{dt} \left( W(g(t)) (t+C)^{-3/4} \right) \leq -4\pi (t+C)^{-3/4}$$

and integrate to get

$$(20.14) \quad (T+C)^{-3/4} W(g(T)) \leq C^{-3/4} W(g(0)) - 16\pi \left[ (T+C)^{1/4} - C^{1/4} \right].$$

Since  $W \geq 0$  by definition and the right hand side of (20.14) would become negative for  $T$  sufficiently large we get the claim.

As a corollary of this theorem we get finite extinction time for the Ricci flow.

**Corollary 20.5.** *Let  $M^3$  be a homotopy 3-sphere equipped with a Riemannian metric  $g = g(0)$ . Under the Ricci flow  $g(t)$  must become extinct in finite time.*

#### REFERENCES

- [1] W. Allard, *On the first variation of a varifold*, Ann. of Math. (2) 95 (1972) 417–491.
- [2] F. J. Almgren, Jr., *Some interior regularity theorems for minimal surfaces and an extension of Bernstein’s theorem*, Ann. of Math. (2) 84 (1966) 277–292.
- [3] F. J. Almgren, Jr., *Almgren’s big regularity paper.  $Q$ -valued functions minimizing Dirichlet’s integral and the regularity of area-minimizing rectifiable currents up to codimension 2*, With a preface by Jean E. Taylor and Vladimir Scheffer. World Scientific Monograph Series in Mathematics, 1. World Scientific Publishing Co., Inc., River Edge, NJ, 2000.
- [4] F. J. Almgren, Jr., *Minimal surface forms*, Math. Intell. 4 (1982) 164–172.

- [5] S. Bernstein, *Über ein geometrisches Theorem und seine Anwendung auf die partiellen Differentialgleichungen vom ellipschen* Typos. Math. Zeit. 26 (1927) 551–558 (translation of the original version in Comm. Soc. Math. Kharkov 2-ème sér. 15 (1915–17) 38–45).
- [6] L. Bers, *Isolated singularities of minimal surfaces*, Ann. of Math. (2) 53 (1951) 364–386.
- [7] G.P. Bessa, L. Jorge and G. Oliveira-Filho, *Half-space theorems for minimal surfaces with bounded curvature*, J. Diff. Geom. 57 (2001) 493–508.
- [8] E. Bombieri, E. De Giorgi, and E. Giusti, *Minimal cones and the Bernstein problem*, Invent. Math. 7 (1969) 243–268.
- [9] H. Bray, *Proof of the Riemannian Penrose inequality using the positive mass theorem*, J. Differential Geom. 59 (2001), no. 2, 177–267.
- [10] E. Calabi, *Problems in differential geometry*, Ed. S. Kobayashi and J. Eells, Jr., *Proceedings of the United States-Japan Seminar in Differential Geometry, Kyoto, Japan, 1965*. Nippon Hyoronsha Co., Ltd., Tokyo (1966) 170.
- [11] S.S. Chern, *The geometry of G-structures*, Bull. Amer. Math. Soc. 72 (1966) 167–219.
- [12] H.I. Choi and R. Schoen, *The space of minimal embeddings of a surface into a three-dimensional manifold of positive Ricci curvature*, Invent. Math. 81 (1985) 387–394.
- [13] T.H. Colding and C. De Lellis, *The min-max construction of minimal surfaces*, Surveys in differential geometry, Vol. 8, Lectures on Geometry and Topology held in honor of Calabi, Lawson, Siu, and Uhlenbeck at Harvard University, May 3–5, 2002, Sponsored by the Journal of Differential Geometry, (2003) 75–107, math.AP/0303305.
- [14] T.H. Colding and W.P. Minicozzi II, *Minimal surfaces*, *Courant Lecture Notes in Math.*, v. 4, 1999.
- [15] T.H. Colding and W.P. Minicozzi II, *Estimates for parametric elliptic integrands*, International Mathematics Research Notices, no. 6 (2002) 291–297.
- [16] T.H. Colding and W.P. Minicozzi II, *The space of embedded minimal surfaces of fixed genus in a 3-manifold I; Estimates off the axis for disks*, Annals of Math., 160 (2004) 27–68, math.AP/0210106.
- [17] T.H. Colding and W.P. Minicozzi II, *The space of embedded minimal surfaces of fixed genus in a 3-manifold II; Multi-valued graphs in disks*, Annals of Math., 160 (2004) 69–92, math.AP/0210086.
- [18] T.H. Colding and W.P. Minicozzi II, *The space of embedded minimal surfaces of fixed genus in a 3-manifold III; Planar domains*, Annals of Math., 160 (2004) 523–572, math.AP/0210141.
- [19] T.H. Colding and W.P. Minicozzi II, *The space of embedded minimal surfaces of fixed genus in a 3-manifold IV; Locally simply connected*, Annals of Math., 160 (2004) 573–615, math.AP/0210119.
- [20] T.H. Colding and W.P. Minicozzi II, *The space of embedded minimal surfaces of fixed genus in a 3-manifold V; Fixed genus*, math.DG/0509647.
- [21] T.H. Colding and W.P. Minicozzi II, *Multi-valued minimal graphs and properness of disks*, International Mathematics Research Notices, no. 21 (2002) 1111–1127.
- [22] T.H. Colding and W.P. Minicozzi II, *On the structure of embedded minimal annuli*, International Mathematics Research Notices, no. 29 (2002) 1539–1552.
- [23] T.H. Colding and W.P. Minicozzi II, *Disks that are double spiral staircases*, Notices of the AMS, Vol. 50, no. 3, March (2003) 327–339.
- [24] T.H. Colding and W.P. Minicozzi II, *Embedded minimal disks: Proper versus nonproper - global versus local*, Transactions of the AMS, 356 (2004) 283–289, math.DG/0210328.
- [25] T.H. Colding and W.P. Minicozzi II, *Estimates for the extinction time for the Ricci flow on certain 3-manifolds and a question of Perelman*, JAMS, 18 (2005), no. 3, 561–569, math.AP/0308090.
- [26] T.H. Colding and W.P. Minicozzi II, *Examples of embedded minimal tori without area bounds*, International Mathematics Research Notices, 99 no. 20 (1999) 1097–1100.
- [27] T.H. Colding and W.P. Minicozzi II, *Complete properly embedded minimal surfaces in  $\mathbf{R}^3$* , Duke Math. J. 107 (2001) 421–426.
- [28] T.H. Colding and W.P. Minicozzi II, *Embedded minimal disks*, Global theory of minimal surfaces, 405–438, Clay Math. Proc., 2, Amer. Math. Soc., Providence, RI, 2005, math.DG/0206146.
- [29] T.H. Colding and W.P. Minicozzi II, *The Calabi-Yau conjectures for embedded surfaces*, preprint, math.DG/0404197.

- [30] P. Collin, *Topologie et courbure des surfaces minimales proprement plongées de  $\mathbf{R}^3$* , Ann. of Math. (2) 145 (1997) 1–31.
- [31] E. De Giorgi, *Frontiere orientate di misura minima*, Sem. Mat. Scuola Norm. Sup. Pisa (1961) 1–56.
- [32] B. Dean, *Compact Embedded Minimal Surfaces of Positive Genus Without Area Bounds*, Geom. Ded. 102 (2003), 45–52.
- [33] T. Ekhholm, B. White, and D. Wienholtz, *Embeddedness of minimal surfaces with total boundary curvature at most  $4\pi$* , Ann. of Math. (2) 155 (2002), no. 1, 209–234.
- [34] H. Federer, *Geometric measure theory*, Springer-Verlag, Berlin–Heidelberg–New York, 1969.
- [35] R. Finn, *Capillary surface interfaces*, Notices Amer. Math. Soc. 46 (1999), no. 7, 770–781.
- [36] M.H. Freedman, J. Hass, and P. Scott, *Least area incompressible surfaces in 3-manifolds*, Invent. Math. 71 (1983), no. 3, 609–642.
- [37] A. Fraser, *On the free boundary variational problem for minimal disks*, Comm. Pure Appl. Math. 53 (2000) 931–971.
- [38] R. Gulliver and J. Spruck, *On embedded minimal surfaces*, Ann. of Math. (2) 103 (1976) 331–347; Ann. of Math. (2) 109 (1979) 407–412.
- [39] R. Hardt, D. Kinderlehrer, and F. H. Lin, *The variety of configurations of static liquid crystals*, Variational methods (Paris, 1988), 115–131, Progr. Nonlinear Differential Equations Appl., 4, Birkhuser Boston, Boston, MA, 1990.
- [40] R. Hardt and L. Simon, *Boundary regularity and embedded solutions for the oriented Plateau problem*, Ann. of Math. (2) 110 (1979), no. 3, 439–486.
- [41] E. Heinz, *Über die Lösungen der Minimalflächengleichung*, Nachr. Akad. Wiss. Göttingen Math.–Phys. Kl, II (1952) 51–56.
- [42] D. Hoffman, *Mixing materials and mathematics*, Nature 384 (1996) 28 - 29.
- [43] D. Hoffman and H. Karcher, *Complete embedded minimal surfaces with finite total curvature*, Geometry V (R. Osserman, ed.) Encyclopaedia Math. Sci. 90, Springer-Verlag, New York (1997) 5–93.
- [44] D. Hoffman and W. Meeks III, *A complete embedded minimal surface in  $\mathbf{R}^3$  with genus one and three ends*, J. Diff. Geom. 21 (1985) 109–127.
- [45] D. Hoffman, M. Weber, and M. Wolf, *An embedded genus-one helicoid*, math.DG/0401080.
- [46] D. Hoffman, M. Weber, and M. Wolf, *An embedded genus-one helicoid*, PNAS, November 15, 2005, vol. 102, no. 46.
- [47] G. Huisken and T. Ilmanen, *The inverse mean curvature flow and the Riemannian Penrose inequality*, J. Differential Geom. 59 (2001), no. 3, 353–437.
- [48] T. Ilmanen, *A strong maximum principle for singular minimal hypersurfaces*, Calc. Var. Partial Differential Equations 4 (1996), no. 5, 443–467.
- [49] L. Jorge and F. Xavier, *On the existence of complete bounded minimal surfaces in  $\mathbf{R}^n$* , Bol. Soc. Brasil. Mat. 10 (1979), no. 2, 171–173.
- [50] L. Jorge and F. Xavier, *A complete minimal surface in  $\mathbf{R}^3$  between two parallel planes*, Annals of Math. (2) 112 (1980) 203–206.
- [51] L. Jorge and F. Xavier, *An inequality between the exterior diameter and the mean curvature of bounded immersions*, Math. Zeit. 178 (1981), no. 1, 77–82.
- [52] N. Kapouleas, *Compact constant mean curvature surfaces in Euclidean three-space*, J. Differential Geom. 33 (1991), no. 3, 683–715.
- [53] N. Kapouleas, *Complete constant mean curvature surfaces in Euclidean three-space*, Ann. of Math. (2) 131 (1990), no. 2, 239–330.
- [54] N. Kapouleas, *Complete embedded minimal surfaces of finite total curvature*, J. Diff. Geom., 47 (1997) 95–169.
- [55] N. Korevaar and R. Kusner, *The global structure of constant mean curvature surfaces*, Invent. Math. 114 (1993), no. 2, 311–332.
- [56] H. B. Lawson, *Lectures on minimal submanifolds*, vol. I, Publish or Perish, Inc, Berkeley, 1980.
- [57] F. Lopez, F. Martin, and S. Morales, *Adding handles to Nadirashvili’s surfaces*, J. Diff. Geom. 60 (2002), no. 1, 155–175.
- [58] F. Lopez, F. Martin, and S. Morales, *Complete nonorientable minimal surfaces in a ball of  $\mathbf{R}^3$* , preprint.
- [59] F. Lopez and A. Ros, *On embedded complete minimal surfaces of genus zero*, J. Differential Geom. 33 (1991), no. 1, 293–300.



- [60] F. Martin and S. Morales, *A complete bounded minimal cylinder in  $\mathbf{R}^3$* , Michigan Math. J. 47 (2000), no. 3, 499–514.
- [61] F. Martin and S. Morales, *On the asymptotic behavior of a complete bounded minimal surface in  $\mathbf{R}^3$* , Trans. Amer. Math. Soc. 356 (2004), 3985–3994.
- [62] F. Martin and S. Morales, *Complete proper minimal surfaces in convex bodies of  $\mathbf{R}^3$* , Duke Math. J. 128 (2005), no. 3, 559–593.
- [63] R. Mazzeo, F. Pacard, and D. Pollack, *Connected sums of constant mean curvature surfaces in Euclidean 3 space*, J. Reine Angew. Math. 536 (2001), 115–165.
- [64] W. Meeks III, *The regularity of the singular set in the Colding and Minicozzi lamination theorem*, Duke Math. Jour., 123 (2004), no. 2, 329–334.
- [65] W. Meeks III, *The lamination metric for the Colding-Minicozzi minimal lamination*, Illinois J. Math. 49 (2005), no. 2, 645–658.
- [66] W. Meeks III and J. Perez, *Conformal properties in classical minimal surface theory*, Surveys in Diff. Geom. IX: Eigenvalues of Laplacians and other geometric operators, Ed. by A. Grigor'yan and S.T. Yau, International Press (2004), 275–335.
- [67] W. Meeks III, J. Perez, and A. Ros, *The geometry of minimal surfaces of finite genus I; Curvature estimates and quasiperiodicity*, J. Differential Geom. 66 (2004), 1–45.
- [68] W. Meeks III, J. Perez, and A. Ros, *The geometry of minimal surfaces of finite genus II; Nonexistence of one limit end examples*, Invent. Math. 158 (2004), no. 2, 323–341.
- [69] W. Meeks III, J. Perez, and A. Ros, *The geometry of minimal surfaces of finite genus III; bounds on the topology and index of classical minimal surfaces*, preprint.
- [70] W. Meeks III and H. Rosenberg, *The uniqueness of the helicoid and the asymptotic geometry of properly embedded minimal surfaces with finite topology*, Ann. of Math., 161 (2005), no. 2, 727–758.
- [71] W. Meeks III and H. Rosenberg, *The minimal lamination closure theorem*, preprint.
- [72] W. Meeks III, L. Simon, and S.T. Yau, *Embedded minimal surfaces, exotic spheres and manifolds with positive Ricci curvature*, Ann. of Math. (2) 116 (1982) 621–659.
- [73] W. Meeks III and M. Weber, *Existence of bent helicoids and the regularity of the singular set in the Colding-Minicozzi lamination theorem*, in preparation.
- [74] W. Meeks III and S.T. Yau, *The classical Plateau problem and the topology of three dimensional manifolds*, Topology 21 (1982) 409–442.
- [75] W.H. Meeks and S.T. Yau, *Topology of three-dimensional manifolds and the embedding problems in minimal surface theory*, Ann. of Math. (2) 112 (1980), no. 3, 441–484.
- [76] M.J. Micallef and J.D. Moore, *Minimal two-spheres and the topology of manifolds with positive curvature on totally isotropic two-planes*, Ann. of Math. (2) 127 (1988) no. 1 199–227.
- [77] N. Nadirashvili, *Hadamard's and Calabi-Yau's conjectures on negatively curved and minimal surfaces*, Invent. Math. 126 (1996) 457–465.
- [78] N. Nadirashvili, *An application of potential analysis to minimal surfaces*, Mosc. Math. J. 1 (2001), no. 4, 601–604, 645.
- [79] R. Osserman, *A survey of minimal surfaces*, Dover, 2nd. edition (1986).
- [80] G. Perelman, *Finite extinction time for the solutions to the Ricci flow on certain three-manifolds*, math.DG/0307245.
- [81] J. Perez, *Limits by rescalings of minimal surfaces: Minimal laminations, curvature decay and local pictures, notes for the workshop "Moduli Spaces of Properly Embedded Minimal Surfaces"*, American Institute of Mathematics, Palo Alto, California (2005).
- [82] J.T. Pitts, *Existence and regularity of minimal surfaces on Riemannian manifolds*, Princeton University Press, Princeton, N.J.; University of Tokyo Press, Tokyo (1981).
- [83] J.T. Pitts and J.H. Rubinstein, *Applications of minmax to minimal surfaces and the topology of 3-manifolds*, Miniconference on geometry and partial differential equations, Proceedings of the CMA, Australia National University (1986).
- [84] H. Rosenberg, *Some recent developments in the theory of properly embedded minimal surfaces in  $\mathbf{R}^3$* , Seminare Bourbaki 1991/92, Asterisque No. 206 (1992) 463–535.
- [85] H. Rosenberg, *Some recent developments in the theory of minimal surfaces in 3-manifolds*, IMPA Mathematical Publications. 24th Brazilian Mathematics Colloquium, Instituto de Matematica Pura e Aplicada (IMPA), Rio de Janeiro, 2003.
- [86] H. Rosenberg, *A complete embedded minimal surface in  $\mathbf{R}^3$  of bounded curvature is proper*, preprint.



- [87] J. Sacks and K. Uhlenbeck, *The existence of minimal immersions of 2-spheres*, Ann. of Math. (2) 113 (1981) no. 1, 1–24.
- [88] R. Schoen, *Estimates for stable minimal surfaces in three-dimensional manifolds*, In Seminar on Minimal Submanifolds, Ann. of Math. Studies, vol. 103, Princeton University Press, Princeton, N.J., (1983) 111–126.
- [89] R. Schoen, *Uniqueness, symmetry, and embeddedness of minimal surfaces*, J. Differential Geom. 18 (1983), no. 4, 791–809 (1984).
- [90] R. Schoen and L. Simon, *Regularity of simply connected surfaces with quasi-conformal Gauss map*, In Seminar on Minimal Submanifolds, Annals of Math. Studies, vol. 103, Princeton University Press, Princeton, N.J., (1983) 127–145.
- [91] R. Schoen, L. Simon, and S.T. Yau, *Curvature estimates for minimal hypersurfaces*, Acta Math. 134 (1975) 275–288.
- [92] Schoen, R. and Yau, S. T., *On the proof of the positive mass conjecture in general relativity*, Comm. Math. Phys. 65 (1979), no. 1, 45–76.
- [93] R. Schoen and S.T. Yau, *Existence of incompressible minimal surfaces and the topology of three dimensional manifolds with nonnegative scalar curvature*, Ann. of Math. (2) 110 (1979) 127–142.
- [94] L. Simon, *Asymptotic behaviour of minimal graphs over exterior domains*, Ann. Inst. H. Poincaré Anal. Non Linéaire 4 (1987) 231–242.
- [95] L. Simon, *Remarks on curvature estimates for minimal hypersurfaces*, Duke Math. J. 43 (1976) 545–553.
- [96] L. Simon, *Singularities of Geometric Variational Problems*, In Nonlinear Partial Differential Equations in Differential Geometry (R. Hardt and M. Wolf, Ed.), American Mathematical Society, Providence (1996) 185–223.
- [97] L. Simon, *A strict maximum principle for area minimizing hypersurfaces*, J. Differential Geom. 26 (1987), no. 2, 327–335.
- [98] J. Simons, *Minimal varieties in Riemannian manifolds*, Ann. of Math. (2) 88 (1968) 62–105.
- [99] F. Smith, *On the existence of embedded minimal 2-spheres in the 3-sphere, endowed with an arbitrary Riemannian metric*, supervisor L. Simon, University of Melbourne (1982).
- [100] B. Solomon and B. White, *A strong maximum principle for varifolds that are stationary with respect to even parametric elliptic functionals*, Indiana Univ. Math. J. 38 (1989), no. 3, 683–691.
- [101] J. Taylor, *Some mathematical challenges in materials science*, Mathematical challenges of the 21st century (Los Angeles, CA, 2000). Bull. Amer. Math. Soc. (N.S.) 40 (2003), no. 1, 69–87.
- [102] D.W. Thompson, *On growth and form*, New ed., Cambridge Univ. Press, Cambridge (1942).
- [103] M. Traizet, *Adding handles to Riemann’s minimal surfaces*, J. Inst. Math. Jussieu 1 (2002) 145–174.
- [104] M. Weber and M. Wolf, *Teichmüller theory and handle addition for minimal surfaces*, Ann. of Math. (2), 156 (2002) 713–795.
- [105] H. Wente, *Counterexample to a conjecture of H. Hopf*, Pacific J. Math. 121 (1986), no. 1, 193–243.
- [106] B. White, *Evolution of curves and surfaces by mean curvature*, Proceedings of the ICM (2002).
- [107] F. Xavier, *Convex hulls of complete minimal surfaces*, Math. Ann. 269 (1984) 179–182.
- [108] S.D. Yang, *A connected sum construction for complete minimal surfaces of finite total curvature*, Comm. Anal. Geom. 9 (2001), no. 1, 115–167.
- [109] S.T. Yau, *Nonlinear analysis in geometry*, L’Eseignement Mathématique (2) 33 (1987) 109–158.

DEPARTMENT OF MATHEMATICS, MIT, 77 MASS. AVE., CAMBRIDGE, MA 02139

DEPARTMENT OF MATHEMATICS, JOHNS HOPKINS UNIVERSITY, 3400 N. CHARLES ST., BALTIMORE, MD 21218

*E-mail address:* [colding@cims.nyu.edu](mailto:colding@cims.nyu.edu) and [minicozz@math.jhu.edu](mailto:minicozz@math.jhu.edu)